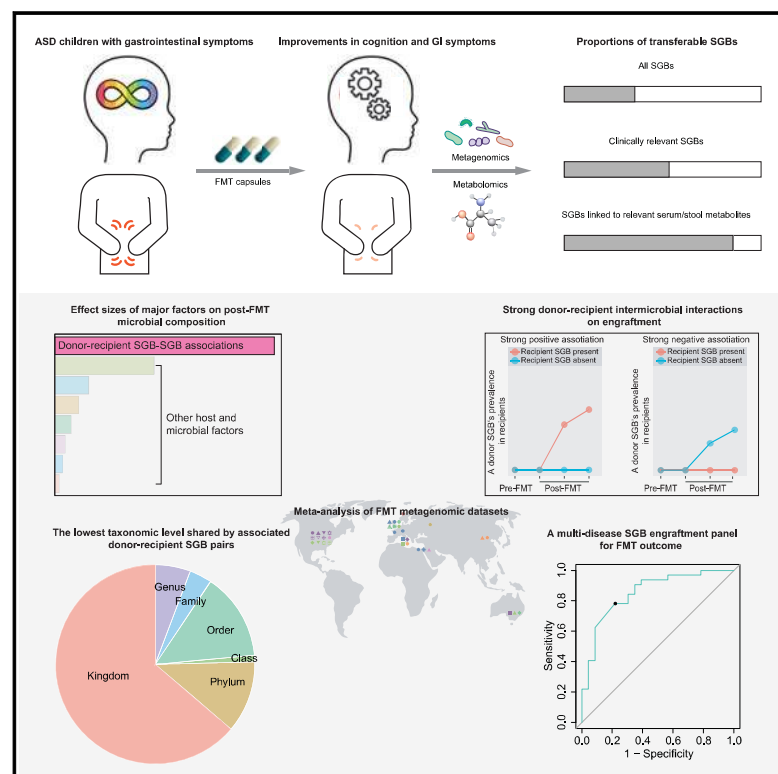


Cell Host & Microbe

Donor-recipient intermicrobial interactions impact transfer of subspecies and fecal microbiota transplantation outcome

Graphical abstract



Authors

Qiyi Chen, Chunyan Wu, Jinfeng Xu, ..., Ning Li, Qian Xu, Huanlong Qin

Correspondence

liningrigs@vip.sina.com (N.L.),
uncqxu@gmail.com (Q.X.),
qinhuanlong@tongji.edu.cn (H.Q.)

In brief

Chen et al. investigate subspecies-level microbiome dynamics using species genome bin in autism spectrum disorder patients undergoing FMT. They discover crucial roles for interactions between subspecies-level entities from donors and recipients on effective microbiota transfer and clinical outcomes. These ecodynamics are shared by FMT datasets across multiple diseases.

Highlights

- FMT displays efficacy in ASD children with gastrointestinal comorbidities
- A donor-recipient SGB match suggests a high likelihood of genuine strain transfer
- Donor-recipient intermicrobial interactions are crucial for microbiota transfer
- Associated donor-recipient SGB pairs generally are phylogenetically divergent

Article

Donor-recipient intermicrobial interactions impact transfer of subspecies and fecal microbiota transplantation outcome

Qiyi Chen,^{1,2,7} Chunyan Wu,^{2,4,7} Jinfeng Xu,^{2,7} Chen Ye,^{1,7} Xiang Chen,⁴ Hongliang Tian,¹ Naixin Zong,² Shaoyi Zhang,⁵ Long Li,¹ Yuan Gao,² Di Zhao,¹ Xiaoqiong Lv,¹ Qilin Yang,³ Le Wang,¹ Jiaqu Cui,¹ Zhiliang Lin,¹ Jubao Lu,¹ Rong Yang,⁶ Fang Yin,² Nan Qin,^{2,4} Ning Li,^{1,*} Qian Xu,^{2,3,8,*} and Huanlong Qin^{1,2,3,*}

¹Department of Colorectal Disease, Intestinal Microenvironment Treatment Center, Shanghai Tenth People's Hospital, Tongji University School of Medicine, Shanghai 200072, China

²Institute of Gut Microbiota Research and Engineering Development, Shanghai Tenth People's Hospital, Tongji University School of Medicine, Shanghai 200072, China

³Institute of Intestinal Diseases, Department of General Surgery, Shanghai Tenth People's Hospital, Tongji University School of Medicine, Shanghai 200072, China

⁴Realbio Genomics Institute, Shanghai 200050, China

⁵Department of Medicine, University of California San Francisco, San Francisco, CA, USA

⁶Department of Pediatrics, Shanghai Tenth People's Hospital, Tongji University School of Medicine, Shanghai 200072, China

⁷These authors contributed equally

⁸Lead contact

*Correspondence: liningrigs@vip.sina.com (N.L.), uncqxu@gmail.com (Q.X.), qinhuanlong@tongji.edu.cn (H.Q.)
<https://doi.org/10.1016/j.chom.2024.01.013>

SUMMARY

Studies on fecal microbiota transplantation (FMT) have reported inconsistent connections between clinical outcomes and donor strain engraftment. Analyses of subspecies-level crosstalk and its influences on lineage transfer in metagenomic FMT datasets have proved challenging, as single-nucleotide polymorphisms (SNPs) are generally not linked and are often absent. Here, we utilized species genome bin (SGB), which employs co-abundance binning, to investigate subspecies-level microbiome dynamics in patients with autism spectrum disorder (ASD) who had gastrointestinal comorbidities and underwent encapsulated FMT (Chinese Clinical Trial: 2100043906). We found that interactions between donor and recipient microbes, which were overwhelmingly phylogenetically divergent, were important for subspecies transfer and positive clinical outcomes. Additionally, a donor-recipient SGB match was indicative of a high likelihood of strain transfer. Importantly, these ecodynamics were shared across FMT datasets encompassing multiple diseases. Collectively, these findings provide detailed insight into specific microbial interactions and dynamics that determine FMT success.

INTRODUCTION

A variety of diseases exhibit abnormalities in gut microbiota,¹ which is in line with the emergence of donor material transfer as a therapeutic option,² although the association between strain engraftment and treatment efficacy remains uncertain and varies among diseases.^{3–5} To date, clinical trials of fecal microbiota transplantation (FMT) have been and are being conducted for a growing list of medical conditions comprising chronic infections, metabolic diseases, malignancies, and neurological disorders, but clinically approved therapy is limited to recurrent *Clostridium difficile* infection (rCDI), suggesting that greater understanding on the deterministic factors of microbiota transfer is needed to unlock the potential.

Given the intricate crosstalk between the central nerve system and gastrointestinal (GI) tract known as the brain-gut axis that

entails gut microbiome components,⁶ several neurological disorders hitherto lacking effective remedies, including autism spectrum disorder (ASD), are being investigated as conditions treatable with FMT.^{7,8} ASD comprises a range of childhood-onset developmental conditions that share impaired social communications and repetitive, purposeless behaviors and have roots in neurological malfunctions.^{9–11} Its prevalence in children is around 1% and exhibits a rising trend in industrialized and emerging countries.^{12,13} Despite the heavy socioeconomic cost, its etiology remains inadequately understood, accompanying the generally moderate-to-poor treatment responses.^{14,15} Although primarily a neuropsychiatric disorder, ASD features a substantial comorbidity rate of GI symptoms,^{16,17} consistent with its associated gut microbiota alterations in humans^{18–20} and the microbiota-coupled mechanistic underpinning of autism-like behaviors in mice.^{21,22}

It has been reported that FMT confers beneficial outcomes to ASD patients in both the core symptoms and GI comorbidities, which are pertinent to microbiota changes.^{23–25} However, these studies do not present subspecies- or strain-level characterization and thus generate limited insights for potentially important microbiome components and events. As a microbial species often comprises functionally distinct lineages,^{26,27} examination of subspecies-level microbiome dynamics is instrumental to elucidate the clinically relevant features,^{4,28} which in metagenomic datasets can be surveyed mainly with two methods, namely single-nucleotide polymorphism (SNP)-resolved differentiation on top of reference-based species assignment²⁹ and co-abundance binning.³⁰ Thus far, studies have shown that engraftment of strains in recipients is influenced by multiple factors, including antibiotic pretreatment, FMT route, and donor and recipient microbial compositions.^{3–5,23} From an ecological perspective, colonization of incoming strains is also dependent on their interactions with local community members,^{3,31} but this question remains insufficiently investigated in FMT metagenomic datasets. This is in part because SNP-based haplotyping, the commonly used approach for metagenomics-based strain inference,^{4,28,32–36} delineates a strain from a panel of polymorphic sites affiliated with a consensus genome. In the context of short-read sequencing that scans a complex community, it is difficult to link distantly located individual SNPs on a reference chromosome, which confuses computational separation of conspecific members (that is, SNP-interpreted strains in a species are generally not stand-alone entities with an abundance metric). Nevertheless, the problem can be avoided by adopting the co-abundance clustering-based reconstruction,^{30,37} such as species genome bins (SGBs), as a subspecies-level proxy. The latest findings based on SGB profiling identify a large group of previously uncharacterized gut bacteria associated with cardiometabolic health.³⁸ Here, we perform an open-label clinical study to investigate the efficacy of FMT for ASD children with GI symptoms, who are subjected to metagenomic and metabolomic analyses, including SGB-based subspecies-level profiling.³⁰ Our findings reveal that effective microbiota transfer involves extensive interactions between donor and recipient microbes that in general are phylogenetically divergent and comprise large proportions of unnamed microbes, and the properties are general across metagenomic datasets of FMT despite tremendous cohort heterogeneity. Hence, interactions between donor and recipient microbes are an ecodynamic force that is crucial for FMT in multiple diseases manifesting gut microbiota perturbations.

RESULTS

Therapeutic responses of ASD patients to FMT

In this open-label study of ASD, we recruited a cohort comprising 29 patients at 2–11 years old and 36 age/sex-matched healthy controls (Figure 1A; Table S1). The patients were enlisted on the basis of meeting the diagnostic standards described in the Diagnostic and Statistical Manual of Mental Disorders (DSM-5-TR), the presence of GI comorbidities, and the absence of several brain, mental, GI, and metabolic diseases (STAR Methods). The ASD patients, who received no pretreatments such as antibiotics or laxatives, underwent a 4-month FMT

regimen of 4-session, oral administration of freeze-dried microbiota capsules. Each monthly session began with clinical assessments, followed by 12-day oral administration commencing on the same or next day that delivered bacterial cells equivalent to that of 200 g fresh stool; ca. 2 weeks after the entire therapy, a follow-up visit was paid to each patient to conduct final clinical scoring^{39,40} (Figure 1B). Our results revealed that the treatment was accompanied by gradual improvements in cognitive deficiency, evidenced by scores of Autistic Behavior Checklist (ABC) scale and Childhood Autism Rating Scale (CARS), and GI symptoms, assessed by Bristol stool scale (BSFS) and Gastrointestinal Symptom Rating Scale (GSRS) ($p < 0.05$, Wilcoxon rank-sum test, Figure 1C). Further scrutinization in individual items of ABC and GSRS illustrated that the therapeutic effects were detected in all aspects of cognition but mainly limited to stool consistency, bloating, heart burn, and belching among GI functions (Figure S1). A comparison of the clinical improvements between two age subgroups of 2–4 and 5–11 years showed that the younger individuals exhibited overall better responses (Figures 1B and 1D), primarily in ABC, CARS, and GSRS at 2 and 3 months post-FMT ($p < 0.05$, Wilcoxon rank-sum test), which probably reflected differences in FMT efficacy between the two age subgroups and coincided with gradual increase of colonization resistance during early life.⁴¹ Overall, our results corroborated the connection between gut microbiota changes and ASD and substantiated the therapeutic potential of FMT for the childhood neuropsychiatric condition.

Associations of post-FMT gut microbiome features with clinical indicators of ASD

To examine the link between the FMT and gut microbiome remodeling or clinical outcomes in the ASD patients (Figures 1C and 1D), we first profiled the fecal microbial composition using SGB-based annotation³⁰ with a minimal 50% completeness. Multivariate Association with Linear Model (MaAsLin) analysis⁴² revealed that there were considerable associations between SGBs (Figure 2A) or microbial genes (Figure 2B) and the clinical indicators (false discovery rate [FDR] < 0.1) and that unexpectedly, most were anticorrelations ($\rho < 0$) with clinical improvements. Among the associated taxa with related characterized representatives, there was a predominance of members in *Collinsella* (78 SGBs), an ASD-enriched genus based on previous reports^{43,44} that were supported by our data (Figure S2). The synchronized patterns in their abundance dynamics (Figure S2A) and associations with the clinical indicators (Figure 2A) suggested that they constituted a taxonomic continuum exhibiting concordant pertinence to ASD. As such, we examined their combined relative abundance, which gradually reduced in the ASD patients over the course of treatment ($p < 0.05$, Pearson correlation test, Figure 2C), but the remaining 196 SGBs of the genus without the CARS connection (Figure S2B) did not; the findings, therefore, unraveled a clinically relevant effect of FMT in suppressing a large group of *Collinsella* strains with a negative clinical annotation. Among the remaining clinical outcome-coupled entities, there were 7 SGBs with family-level labels, including 6 from Clostridiaceae and Clostridiales unclassified, and 4 unassigned SGBs, illustrating the clinical implications of gut microbial members having barely been explored. Despite a level of consensus in microbiome associations between the two core

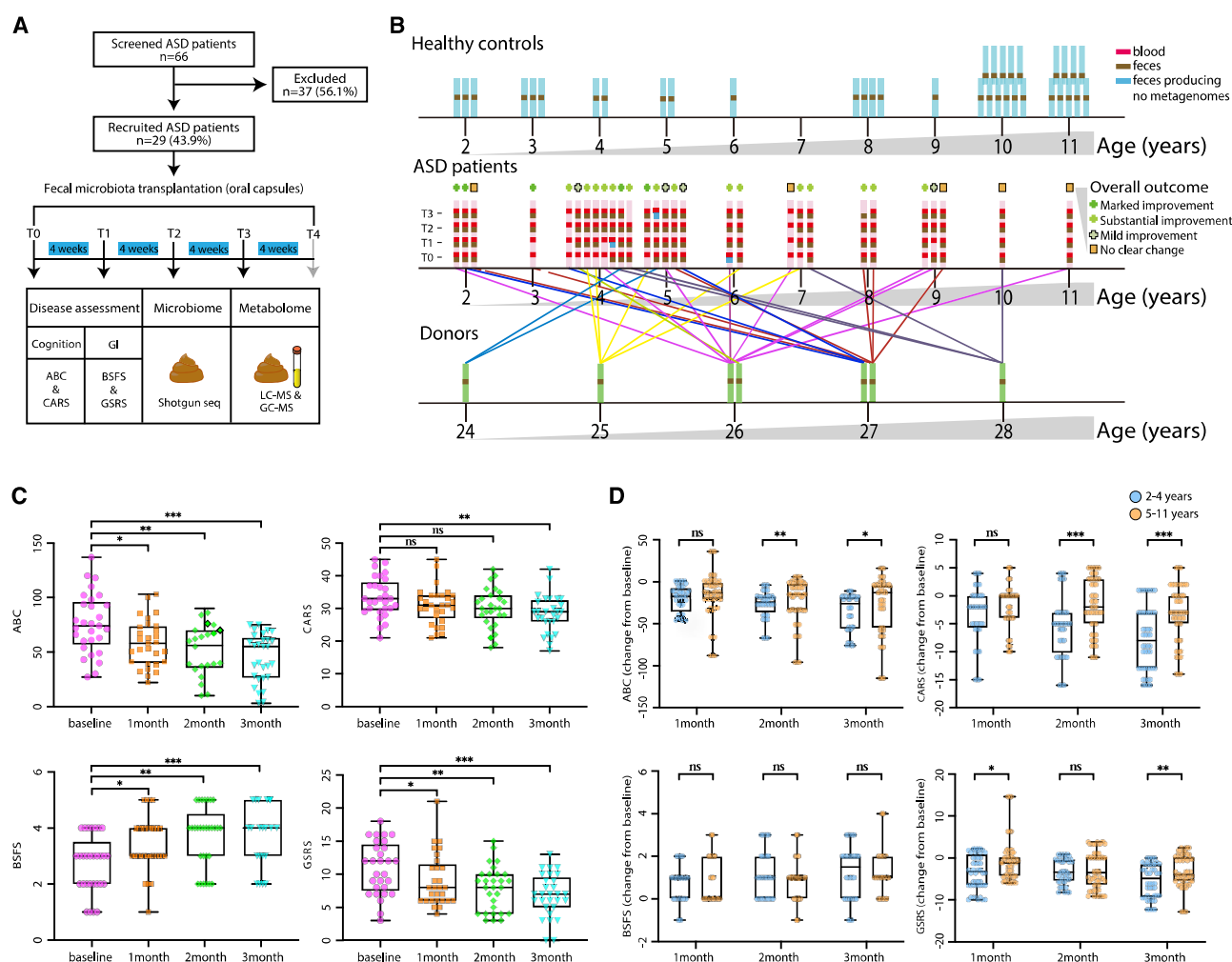


Figure 1. The study design and assessment of cognitive and gastrointestinal functions in ASD patients

(A) The study design of the recruited ASD patients undergoing FMT intervention. Due to reduced patient compliance at T4, there were only 4 stool samples and 1 serum sample at this time point, and the resulting metagenomic/metabolomic source data were not included in the analyses.

(B) FMT setup, clinical outcome, and sampling of the participants.

(C and D) Clinical assessment of the ASD patients (C) and the two age subgroups (D, change from baseline) during the course of FMT treatment (*p < 0.05, **p < 0.01, ***p < 1 × 10⁻³, Wilcoxon rank-sum test). Box edges correspond to lower and upper quartiles, whereas the center line denotes the median, and whiskers extend to 1.5 times the interquartile range (IQR).

ASD indicators, the number of CARS connections was over 7-fold of that of ABC, indicating divergent sensitivity in capturing relevant features that concurred with the superior accuracy of CARS in diagnosing the disorder.^{45,46}

We defined a donor-to-recipient transfer event as a newly arisen feature in a post-FMT recipient matched to the donor and found that transferable SGBs and KEGG orthologs (KOs), or features displaying at least one transfer event, accounted for 35.8% and 28.9% of total identified taxa and genes and that the corresponding ratios showed noticeable gain (53.3% and 46.5%) in the CARS/ABC/BSFS/GSRS-associated features (Figure 2D). As exemplified by the *Collinsella* SGBs pertinent to the ASD indicators, the microbiome features with donor-to-recipient transfer events could be disease-associated but displayed depletion over the course of treatment; the ratio of transferable SGBs in *Collinsella* (28%) was on par with other

top genera including *Clostridium*, *Streptococcus*, and *Prevotella* (38%–68%), which conformed to relatively good transferability of donor strains from high-proportion species.³ The finding deviated from a conventionally perceived working model of FMT (that is, transfer of beneficial microbes to recipients) and implied inter-microbial competition initiated by the introduction of donor microbiota. As the abundance values of these *Collinsella* SGBs in the donors were mostly numerically below that in the corresponding pre-FMT recipients, with 34 SGBs reaching statistical significance (p < 0.01, donors vs. recipients at T0, Wilcoxon rank-sum test, Figure S2), we wondered a possibility of dual origins of many CARS-associated *Collinsella* SGBs in the post-FMT recipients, with minor donor contribution. This was supported by tracing of SNPs specific to donors and pre-FMT recipients (Figure 2E). Interestingly, the SNP source disparity dissipated in recipients at 3 months post-FMT, congruent with the

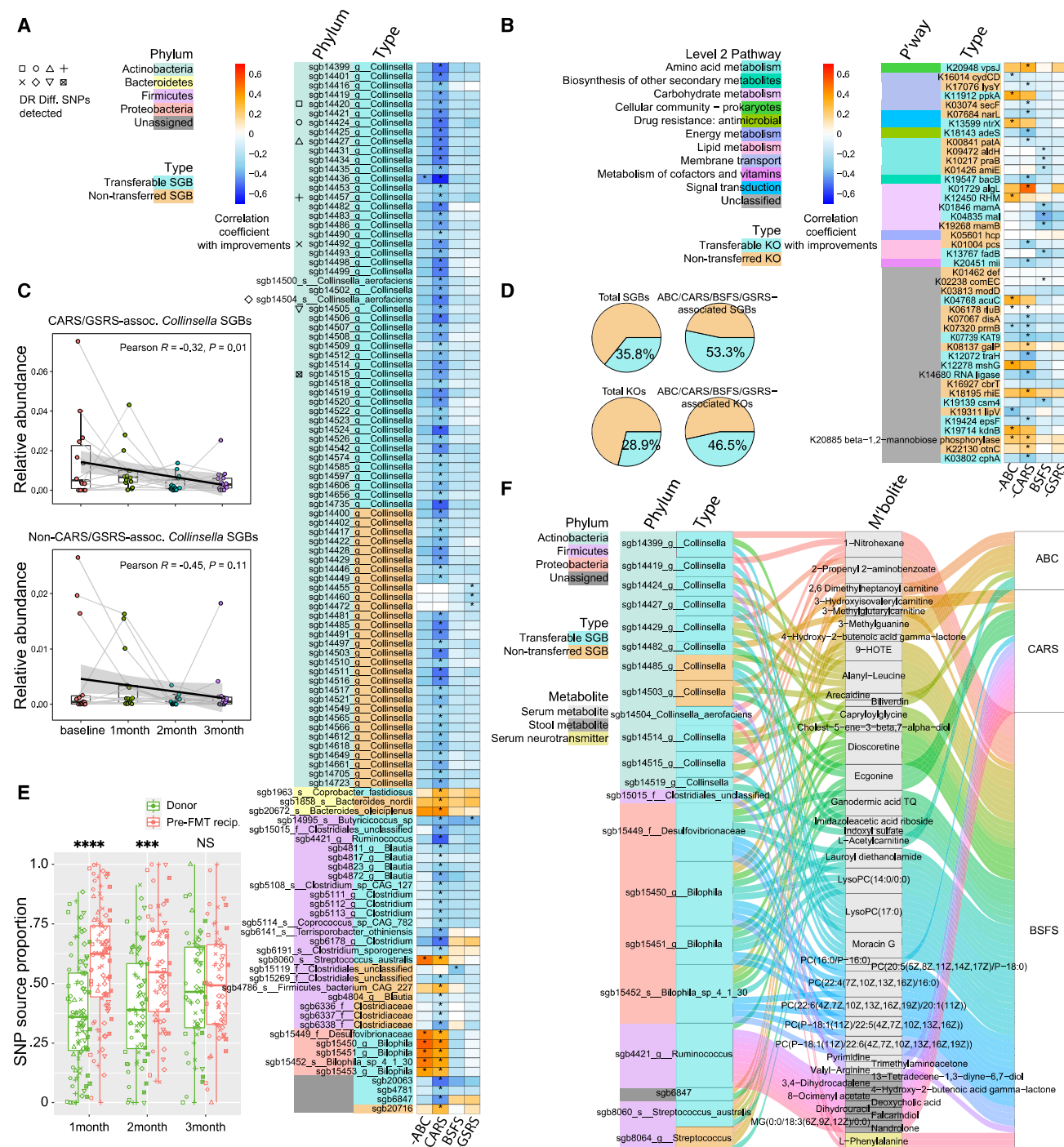


Figure 2. Association of gut microbiome features with the clinical indicators of ASD

(A and B) Associations of gut microbiome SGBs (A) and KOs (B) with clinical improvements (negative values of ABC, CARS, and GSRS and positive value of BSFS) of core ASD symptoms or GI comorbidities based on Multivariate Association with Linear Model (MaAsLin) analysis (*FDR < 0.1). The *Collinsella* SGBs with SNPs specific to donors or pre-FMT recipients are marked by symbols. These SNPs are not in marker genes employed by StrainPhlAn⁴⁷; SNPs in marker genes were not detected for transferable *Collinsella* SGBs.

(C) Correlation of the combined relative abundance of *Collinsella* SGBs with the treatment time points in the 14 ASD patients with complete fecal shotgun data at all four time points (Pearson correlation test); all 78 CARS-associated *Collinsella* SGBs or the 196 remaining *Collinsella* SGBs detected in the ASD cohort are included. Lines connect time point samples from the same individual. The shaded area shows a 95% confidence interval. Box edges correspond to lower and upper quartiles, whereas the center line denotes the median, and whiskers extend to 1.5 times the IQR.

(D) Proportions of the transferable SGBs and KOs to the total or clinical outcome-associated microbiome features in the stool samples of post-FMT ASD patients.

(legend continued on next page)

SNPs not being in marker genes⁴⁷ and possibly underpinning little functional differences. Overall, although carryover of low-level disease-associated strains into recipients is hard to avoid in practice, they may be suppressed over the course of FMT.

Most of the taxonomic and functional associations with the clinical outcome were recorded for CARS and ABC (Figures 2A and 2B), suggesting a considerable impact of FMT-induced microbiome restructuring on neuropsychiatric performance. We reasoned that the microbial alterations might translate into metabolic differences, including some implicated in cognition. The mediation effects of serum metabolites, serum neurotransmitters, and stool metabolites in between the microbes and ASD indicators were examined, showing that dozens of compounds bridged the associations (Figure 2F). Among these, serum metabolites of biliverdin,⁴⁸ acetylcarnitine (an intermediate of acetyl coenzyme A [CoA]),⁴⁹ and pyrimidine⁵⁰ and stool metabolites of faltarindiol,⁵¹ deoxycholic acid,⁵² and nandrolone⁵³ have previously shown to associate with neurotransmission. Among the minority of taxonomic entities tied to clinical improvements (Figure 2A), SGB15450_ *Bilophila* and SGB8060_ *Streptococcus australis* exhibited connections to carnitine species, and carnitine deficiency in the brain may play a role in autism.⁵⁴ Moreover, multiple molecules of phosphatidylcholine (PC) and lysoPC were linked to BSFS, consistent with the regulatory roles of these lipids on GI functions.^{55,56} Importantly, over 85% of the SGBs displaying mediation effects were transferable (Figure 2F), corroborating the implications of donor strain engraftment in patients manifesting cognition impairment and gut microbiota deviations.

Influences of DR intermicrobial interactions on lineage transfer

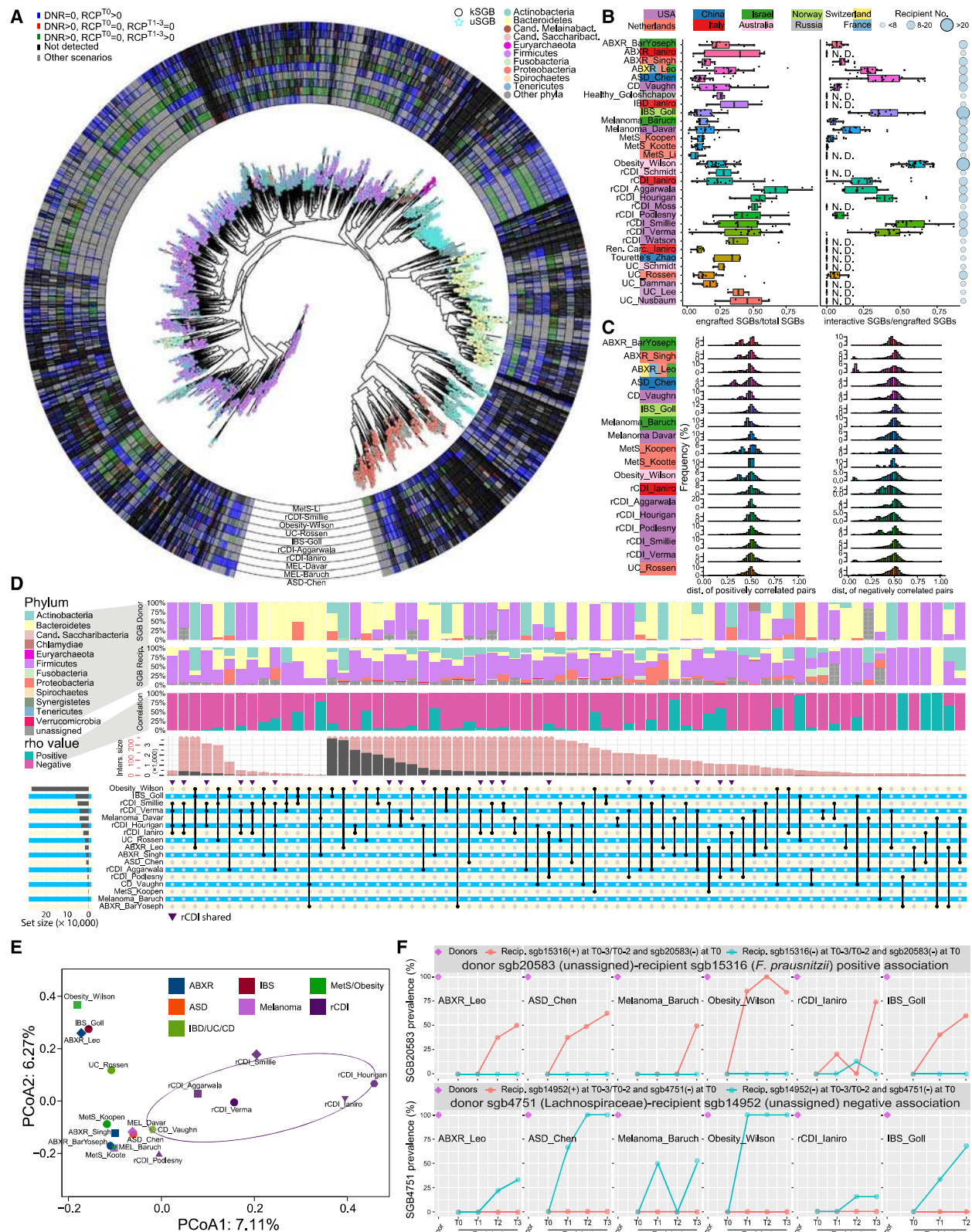
- We hypothesized that during FMT, intermingling between incoming and indigenous strains plays a crucial role in the engraftment and persistence of donor members, and the conjecture was interrogated in a meta-analysis encompassing the in-house ASD cohort and 30 published metagenomic datasets of FMT,^{4,5,28,32–36,57–77} which covered gut microbiota dysbiosis, GI diseases, malignancies, metabolic diseases, and neuropsychiatric diseases (Table S2). Intermicrobial interactions and their impact on strain transfer are underlain by the inherent manner between organisms⁷⁸ that transcends different host medical and demographic conditions. We identified a total of 5,051 SGBs and 3,429 transferable members, among which 2,972 exhibited engraftment in more than one cohort (Figure 3A; Table S3). The SGB profiling (Figure S3A) validated large unclassified diversity within *Collinsella*,⁷⁹ *Prevotella*,⁸⁰ and *Streptococcus*⁸¹ reported previously, and SGBs with species labels constructed in this study exhibited a median sequence similarity of 97.4% to relevant reference genomes (Figure S3A). In addition, 2,434 SGBs were concentrated in 112 genus-level taxa

with ≥ 4 SGBs/taxon (Figures S3B and S3C), which accounted for 70%–80% of total microbiota abundance in each dataset and most hosted larger numbers of detected SGBs than that of validly named species (lpsn.dsmz.de), suggesting that the SGB profiling captured subspecies-level diversity. Notable outliers included: (1) genera of considerable clinical or industrial interest that have been historically subjected to intensive classification efforts and contain many rare species (such as *Pseudomonas*); (2) genera mainly associated with plants or the environment (such as *Sphingomonas*).

- As a quality control for microbiota transfer, about 60% of newly appeared SGBs in recipients at the first post-FMT time point were matched to the corresponding donors (Figure S3D). The traceability deficit might be caused by limited sequencing depth for subspecies-level profiling, many lineages with baseline abundance, and microbiota composition fluctuation in donors (for example, stool collection for FMT and for metagenomic sequencing might occur on different days). The median sequence similarity and SNP identity between matched donor and new post-FMT recipient SGBs (that is, pairs consistent with an FMT connection) were 99.10% and 99.99%, which were both significantly above that between two assemblies of a same label lacking an FMT connection ($p < 2.2 \times 10^{-16}$, Wilcoxon rank-sum test, Figure S3E), indicating that such a match largely reflected genuine strain or ecotype transfer. Engraftment rates, determined as the ratio of transferred SGB numbers to total SGB numbers in post-FMT recipients, displayed apparent variations between datasets (Figures 3A and 3B). Recipients of rCDI, currently the only disease with clinically approved FMT therapy, exhibited higher donor lineage transfer than patients of other diseases (rCDI vs. non-rCDI, $p \leq 2 \times 10^{-16}$, Wilcoxon rank-sum test, Figure S4A) that was in line with previous observation.⁴ This was accompanied by rCDI-coupled elevation in the proportion of transferred SGBs displaying donor-recipient (DR) subspecies-level quantitative-binary associations (FDR < 0.05, $\rho > 0.7$ or < -0.7 , Spearman association analysis based on the relative abundance data of all SGBs in pre-FMT recipients and binary presence-absence data of a donor SGB in post-FMT recipients), defined as correlative SGB numbers normalized by engrafted SGB numbers in post-FMT patients (rCDI vs. non-rCDI, $p \leq 2 \times 10^{-16}$, Wilcoxon rank-sum test; Figure S4A). Of note, the DR connections were detected in 18 cohorts with 9–42 recipients (Table S2), including four medium-size cohorts (8–12 recipients) with baseline results, but were absent in the remaining smaller cohorts (2–7 recipients), suggesting that a minimal sample size of 10 recipients is desirable for confidently assessing interactions between microbes from donors and recipients. Indicative of the clinical implications, quantitative-binary associations with

(E) SNP source (donor vs. pre-FMT recipient) comparison of *Collinsella* SGBs in post-FMT recipients at different time points (*** $p < 1 \times 10^{-3}$, **** $p < 1 \times 10^{-8}$, Wilcoxon rank-sum test). Each symbol represents SNPs of a *Collinsella* SGB marked in (A). Box edges correspond to lower and upper quartiles, whereas the center line denotes the median, and whiskers extend to 1.5 times the IQR.

(F) Parallel coordinates chart showing the mediation links of serum metabolites, stool metabolites, and serum neurotransmitters (FDR < 0.05, mediation analysis) in-between SGBs and ASD indicators. The curved lines connecting the panels indicate the mediation effects, with colors tying to individual metabolites.



(legend on next page)

recipient microbes were detected for three transferable SGBs that were associated with ASD indicators (Figure 2A), namely SGB15015_Clostridiales_unclassified, unassigned SGB20063, and SGB4872_Blaustia. Large genetic distances were found to straddle the incoming and resident strains of both positively and negatively associated pairs (Figure 3C). To put in perspective, 63.7% and 11.7% of the interactive donor and recipient SGBs, if both having phylogenetic labels, shared the affiliations not until at the kingdom and phylum levels, as opposed to only 5.70% and 0.022% at the genus and species levels.

- Substantial consensus was observed in the subspecies-level associations among individual FMT datasets (Figure 3D), coincided with the ordination cluster that different cohorts and disease types converged (Figure 3E), although all 5 rCDI cohorts with at least 9 recipients exhibited concordant departure, attested to disease-specific traits of microbial crosstalk during FMT (Figure 3D). This was paralleled by deviated gut microbiome structures of pre-FMT rCDI patients (Figure S4B) that corroborated a recent study³ and illustrated severe dysbiosis associated with the infection. Large proportions of the interactive entities across datasets were found in Firmicutes and Bacteroides, two dominant phyla in human gut microbiota, as well as in Actinobacteria and unassigned SGBs, two relatively under-appreciated groups. This was in line with the findings that among the DR connections detected in at least 3 cohorts, members of *Collinsella*, an actinobacterial genus, were the top contributors to both donor- and recipient-originated interactive SGBs, followed by lineages of *Faecalibacterium* and *Prevotella* as well as unassigned SGBs. We noted that pre-FMT rCDI patients exhibited significantly lower taxonomic diversity than their non-rCDI counterparts ($p \leq 2 \times 10^{-16}$, Wilcoxon rank-sum test; Figure S4A), which was in agreement with previous findings³ and was reminiscent of gut microbiome dynamics in early childhood,⁴¹ given the concurrently low degrees of taxonomic complexity and colonization resistance. Nevertheless, transfer and retention of a donor SGB tied to the presence of its highly correlative (that is,

with a more stringent rho cutoff; $FDR < 0.05$, $\rho > 0.9$ or < -0.9 , Spearman correlation test) recipient entities were consistently observed in all six cohorts with multiple post-FMT time points and considerable levels of DR inter-microbial associations (Figure 3F; Figure S5).

Coupling between DR intermicrobial interactions and clinical outcome

- We next examined the clinical relevance of DR subspecies-level quantitative-binary associations and donor microbiota engraftment in a multitude of medical conditions by focusing on the transferable features. As revealed by principal-coordinate analysis (PCoA), pre-FMT patients exhibited apparent deviations from the healthy donors both taxonomically and functionally, which were attenuated following the interventions (Figures 4A and 4B). However, such global trajectories of gut microbiome did not account for clinical outcome (responders vs. non-responders). To identify specific donor microbiome descriptors, we analyzed the correlations of SGB or KO transfer with the clinical endpoints and uncovered microbiome entities distinguishing the two groups of recipients in the pooled 19 datasets with responder/non-responder information (Figures 4C and 4D; Table S4; $p < 0.05$, linear discriminant analysis (LDA) > 2.0). There was apparent co-occurrence between taxonomy and clinical relevance, exemplified by uniform associations of all 24 and 71 SGBs in *Fecalibacterium* and Prevotellaceae, respectively, but mixed ties were found in *Clostridium* and *Bifidobacterium*. Of the most discriminating SGBs ($p < 0.05$, LDA > 2.5), members of *Fecalibacterium*, *Bifidobacterium*, *Ruminococcus*, and *Coprococcus* or *Prevotella* had a major presence in responder- or non-responder-associated features, respectively; some of the connections were in line with health association of these genera,^{82–84} but more importantly, the results highlighted specific, rarely investigated lineages possibly important in FMT prognosis. Coincided with the exclusively negative associations of *Collinsella* SGBs with clinical improvements in ASD

Figure 3. SGB engraftment and DR subspecies-level quantitative-binary associations across FMT metagenomic datasets

(A) Phylogeny and transferability of representative genomes from each species-level genome bin (SGB) identified in 31 FMT metagenomic datasets. DNR, donor; RCP, recipient; T0, before FMT; T1–3, different time points after FMT; the color scheme in the rings reflects the pre-FMT and post-FMT averages of donors or recipients of each dataset; intervals vary from a week to a month in individual studies. kSGB, known SGB; uSGB, unknown SGB.

(B) SGB transfer rate and donor-recipient (DR) subspecies-level quantitative-binary associations in different datasets. In box plots, box edges correspond to lower and upper quartiles, whereas the center line denotes the median, and whiskers extend to 1.5 times the IQR. The background color stripe of each dataset indicates the country where the study was conducted. N. D., not detected.

(C) Percentage distribution of Mash-estimated genetic distances of quantitative-binary-associated donor-recipient SGB pairs. In the main peaks of 0.4–0.6 distance, 75.0% and 12.6% or 0.32% and 0.007% of the interactive pairs, if both assigned with taxonomic labels, shared the affiliations not until at the kingdom and phylum levels or genus and species levels, respectively.

(D) UpSet plot showing the number (≥ 5) of donor-recipient subspecies-level quantitative-binary associations shared by combinations of FMT datasets. Two overlapping scales, colored red and black, are used to accommodate the vast differences in intersection sizes. Combinations shared only by rCDI datasets are marked by purple, down-pointing triangles.

(E) Ordination of the donor-recipient quantitative-binary associations in different FMT metagenomic datasets. PCoA was generated using Bray-Curtis distance, which was computed based on the binary data matrix of the DR intermicrobial associations in each dataset. Each symbol represents the subspecies-level associations of a dataset. The ellipse of rCDI datasets depicts their consistent deviation from the cluster where multiple non-rCDI cohorts converge.

(F) Prevalence of unassigned SGB20583 and Lachnospiraceae SGB4751 in FMT donors and recipients of multiple datasets with or without the presence of its highly associated ($\rho > 0.9$ or < -0.9) recipient lineages. Among the seven datasets with multiple post-FMT time points and detectable DR intermicrobial associations, the MetS_Kootte dataset or the other six had 45 or at least 1,195 DR connections, respectively. The results were from the subset of recipients who lacked SGB20583 (top row) or SGB4751 (bottom row) before FMT, as well as their corresponding donors.

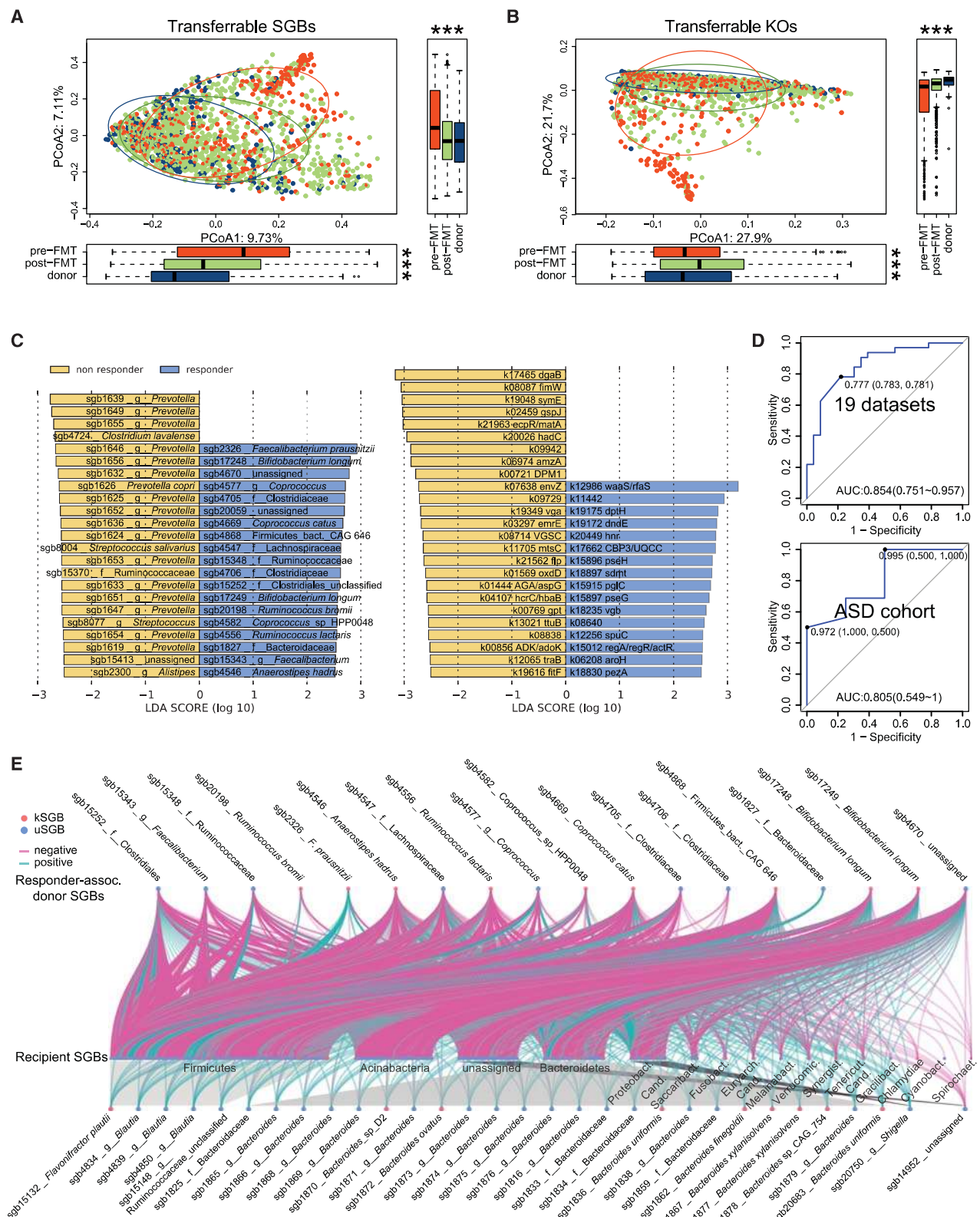


Figure 4. Influence of DR intermicrobial interactions on gut microbiome structure and clinical outcome across FMT metagenomic datasets (A and B) Principal-coordinate analysis (PCoA) of transferable SGBs (A) and KOs (B) in pre-FMT recipients, post-FMT recipients, and donors across FMT metagenomic datasets ($p < 0.01$, analysis of similarities (ANOSIM) test).

(legend continued on next page)

(Figure 2A), there were 4 SGBs of the genus and one from the parent family associated with treatment outcome (Table S4, $p < 0.05$, LDA > 2.0), with all being enriched in non-responders. Among the clinically relevant KOs, non-responder-associated K12065 (*traB*) was coherent with K12072 (*traH*) that was unfavorably tied to a core ASD indicator (Figure 2B); the two conjugal transfer genes were detected in plasmids hosted by *Enterococcus faecium*, *Enterococcus faecalis*, and *Enterobacter ludwigii*, which are being increasingly reported as multidrug resistant nosocomial pathogens. On the other hand, K15896 (*pseH*) and K15897 (*pseG*) underscored the over-representation of O-antigen nucleotide sugar biosynthesis genes in responders. Corroborating the clinical implications, an SGB engraftment panel was able to predict treatment response with good performance in the combined 19 datasets or the in-house ASD cohort (Figure 4D).

- Consistent with the overall DR intermicrobial responses reported in this (Figure 3D) and a previous study,⁴ most of the responder-associated donor SGBs displayed largely negative interactions with recipient microbial communities, including those connecting to SGB14952 that showed extensive engraftment inhibition (Figure 3F), although SGB2326_F. *praeunizii*, SGB1827_Bacteroidaceae, and SGB20059 encountered little colonization resistance (Figure 4E). Despite the general landscape, around 30 recipient SGBs exhibited facilitative responses to the incoming beneficial strains, and most belonged to *Bacteroides*, along with four close relatives in the parent family (Figure 4E). However, there was no association between the abundance of *Bacteroides* in recipients and their clinical responses, reinforcing the necessity of subspecies-level characterization in FMT.

Identification of an unnamed, clinically relevant species prevalent in FMT datasets

Our analyses showed that uncharacterized SGBs were common among clinically relevant taxonomic entities in FMT datasets (Figures 2A, 4C, and 4E). Among these, we found one member in the family of Clostridiaceae, SGB4705, being prevalent (Figure 5A) and exhibiting broad interactions with recipient SGBs (Figure 4E), which represented a distinct species we named *Candidatus Tongjibacter transferonalis*. Genetic distance-based computation indicated that the SGB is a close relative of the genus *Clostridium* but displays a large departure from *Clostridium* species and strains (Figure S6A) such that it merits a separate genus assignment. There were multiple uncharacterized microbes with substantial cross-cohort prevalence in Clostridiaceae (Figure 5B), including two responder-associated SGBs, namely *Ca. T. transferonalis* and SGB4706 (Figure 4C).

This suggested that these microbes, albeit generally at low relative abundances (ca. 0.1% for *Ca. T. transferonalis* in donors and pre-FMT patients), were members of a subtree with considerable relevance in FMT. Given the versatile clinical ties of Clostridiaceae SGBs (that is, 8 SGBs with unfavorable correlations with a core ASD indicator, Figure 2A; 5 responder-associated and 7 non-responder-associated SGBs, $p < 0.05$, LDA > 2 , Figure 4C; Table S4), a better understanding of clades in this family is conducive for bridging the connection between donor microbiota engraftment and treatment outcome in multiple medical conditions. Although there was no evident intra-SGB clustering associated with diseases (Figure 5A), ordination based on genetic distances among metagenome-assembled genomes (MAGs) uncovered two lineages of *Ca. T. transferonalis*, which were mainly found in individuals from China or North America and Europe, corroborating the link between host geography or lifestyle and gut microbe strain variations.³⁰

Despite the close phylogeny and similar cross-cohort associations with clinical outcome, however, *Ca. T. transferonalis* and SGB4706 from donors manifested disparate quantitative-binary associations with recipient SGBs (Figure 5D) that corresponded to minimal colonization resistance encountered by SGB4706, as the intermicrobial responses of both were overwhelmingly suppressive. This was congruent with the differential engraftment efficiency between *Ca. T. transferonalis* and SGB4706, given that SGB4706 had less than one-fifth of the donor relative abundance compared with that of *Ca. T. transferonalis*, but the two SGBs registered comparable counts of engraftment (Figure 5E; Figure S6B). Functional profiling revealed differences between *Ca. T. transferonalis* and SGB4706 in fatty acid metabolism, styrene degradation, and sphingolipid metabolism ($p < 0.01$, Wilcoxon rank-sum test). Because some types of fatty acids and sphingolipids are ingredients of the bacterial cell envelope and can potentially influence microbe-microbe crosstalk, these concurrent differences in intermicrobial interactions and metabolic functions between the two microbes may illuminate key components conferring minimal engraftment resistance.

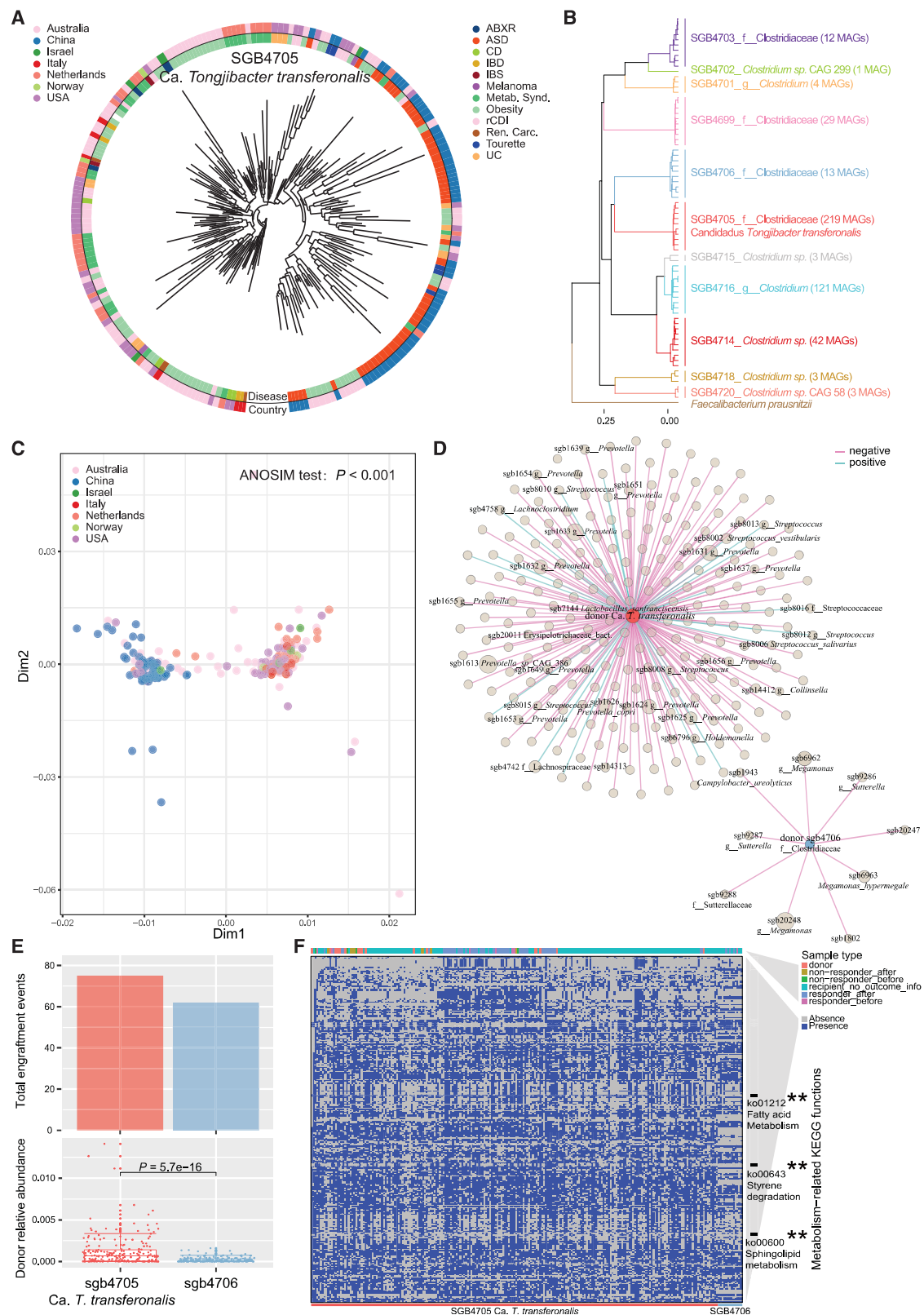
Connection between subspecies-level associations and compositions of subspecies entities

In FMT metagenomic studies, dynamics of SNP-informed strain composition within individual species has been employed to monitor donor microbiota engraftment.^{4,34,36} We sought to assess the relationship between subspecies-level interactions and the composition dynamics of closely related entities. Among multiple clinical and microbiome variables, subspecies-level quantitative-binary associations displayed a prominent impact on donor microbe engraftment (Figure 6A). Moreover, SGBs with over 2-fold post-FMT enrichment or depletion in recipients were tied to significantly greater numbers of associated indigenous lineages (FDR < 0.05 , $\rho > 0.7$ or < -0.7 , Spearman

(C) LefSe analysis of the clinical response of SGB (left) and KO (right) transfer based on 19 FMT metagenomic datasets with available clinical response information.

(D) The receiver operating characteristic (ROC) curve for predicting treatment response based on SGB engraftment generated by random forest.

(E) Significant quantitative-binary associations (FDR < 0.05 , $\rho > 0.7$, or < -0.7 , Spearman correlation test) between the responder-associated donor SGBs (top row) and recipient SGBs (lower rows). The associated recipient SGBs are grouped into phyla or unassigned SGBs, with those with the largest numbers of positive associations (all recipient SGBs with at least 7 positive associations and no more than one negative association) or SGB14952 (showing cross-cohort engraftment inhibition; see Figure 3F) being specified. kSGB, known SGB; uSGB, unknown SGB.



(legend on next page)

correlation test), referred hereafter as association size, than that of SGBs with relative flat abundance curves ($p \leq 2.22 \times 10^{-16}$, Wilcoxon rank-sum test, Figure 6B). A similar pattern was also found in the large repertoire of over 300 members of *Collinsella* (Figure 6C), pointing to the ecological factor potentially contributing to the differential post-FMT kinetics in the genus (Figure 2C). These findings implied that microbe-microbe interplay might impart strain composition changes of a species, which motivated us to examine the abundance dynamics and association size of individual members in multi-SGB bacteria, defined as species with at least two affiliating SGBs detected in this study. Here, quantitative-quantitative association based on relative abundance data of both SGBs (FDR < 0.1, Spearman correlation test, Table S5) was used to assess the microbial interdependence pertinent to conspecific composition.

Intriguingly, although most surveyed SGBs exhibited considerable interpersonal variations in intra-species proportion (Figure 6D; Table S5), integrated results from the donors ($n = 178$) or recipients ($n = 312$) before and after FMT revealed that regardless the differences in association size among closely related members, the conspecific landscape of most multi-SGB bacteria remained largely conserved at the population level (Figure 6E), which was well exemplified by the multiple SGBs in *Actinomyces oris*, *Enterobacter cloacae*, *Streptococcus mitis*, or *Streptococcus oralis*. Exceptions with divergent post-FMT abundance changes of SGBs included SGB17249 and SGB17248 of *Bifidobacterium lognum* (post-FMT fold changes of 0.45 and 1.29, FDR < 0.05) and SGB14630, SGB14504, and SGB14500 of *Collinsella aerofaciens* (post-FMT fold changes of 0.82, 1.52, and 1.87, FDR < 0.05), although the post-FMT composition of either species approached that of donors. Our results implied that for many gut bacteria, there is resilience in strain composition coherent with the unique functional properties of individual members. In addition, there was a drastic post-FMT species-level reduction in many disease-associated bacteria that mostly approached the levels in healthy people, as evidenced by *Citrobacter freundii*, *Providencia rettgeri*, *Veillonella dispar*, and *Klebsiella michiganensis* (FDR < 0.05). Such species-level trajectory is reminiscent of the progressive depletion of the large group of CARS/GSRS-associated *Collinsella* SGBs (Figure 2C), although their taxonomy remains to be fully established. Overall, whereas strain-level interactions play a pivotal role in dictating whether an incoming microbe may colonize a recipient (qualitative change), their influence on the post-FMT abundance of an introduced strain (quantitative change) is constrained by the intra-species composition and species-level dynamics.

DISCUSSION

This study on FMT treatment of ASD patients with GI symptoms represents an early step in investigating the therapy, which currently has highly limited applications, to treat a childhood neuropsychiatric disorder. Our results indicate that the encapsulated delivery yields clinical improvements, that the effect is linked to the transfer of donor materials, and that as demonstrated in a large-scale meta-analysis, subspecies-level interactions constitute a critical determinant for engraftment. One complication in metagenomics-based examination of these intermicrobial activities is the conflict between the biological events that often enlist discrete subspecies entities and canonical strain annotation that relies on marker gene polymorphism and correspondingly produces superposed computational elements. In light of this, binning-based reconstruction, such as SGB, offers an alternative for strain tracking in FMT metagenomics. Our observation reveals that matching of donor and newly arisen post-FMT recipient SGBs is accompanied by a median sequence similarity of 99% and a median SNP identity of 99.99%, which contrast with 5% genetic diversity in each SGB and imply a low likelihood of random microbial dynamics being the cause.

Despite the divergent approaches, our SGB-based analysis aligns with a previous study,⁴ which employs SNP-based strain profiling to show that DR intermicrobial associations are mostly negative. Thus, overcoming colonization resistance by resident microbial communities represents a major avenue to assist engraftment and clinical outcome. Nevertheless, there lies an outstanding discrepancy, as majority of the interactive donor and recipient members may be phylogenetically close⁴ or remote (Figure 3C). The conflicting findings infer different modes of action⁷⁸; in the case of negative interactions, that between two closely related, metabolically analogous microbes may be due to competition for common nutrients, but that between two unrelated ones are possibly driven by metabolic cross-suppression (that is, products by one microbe are detrimental to the other). In addition, during FMT the chance of an incoming microbe getting physically close contact with related kin cells is slim compared with unrelated, diverse bacteria; thus, the two possibilities imply vastly different levels of influence of DR intermicrobial interactions on engraftment. Lastly, the interpretation by Schmidt et al.⁴ suggests that strains with a large number of close relatives may be subjected to greater impact than their counterparts from bacteria harboring low intra-species diversity. A better understanding of the complex interplay during FMT is needed to enhance the degree of causality or predictability in the transfer that has long been regarded as a black-box process.²

Figure 5. Characterization of an unnamed microbe in the family of Clostridiaceae that is prevalent across FMT datasets

(A) Phylogeny of 219 MAGs in *Ca. Tongijibacter transferonalis*.

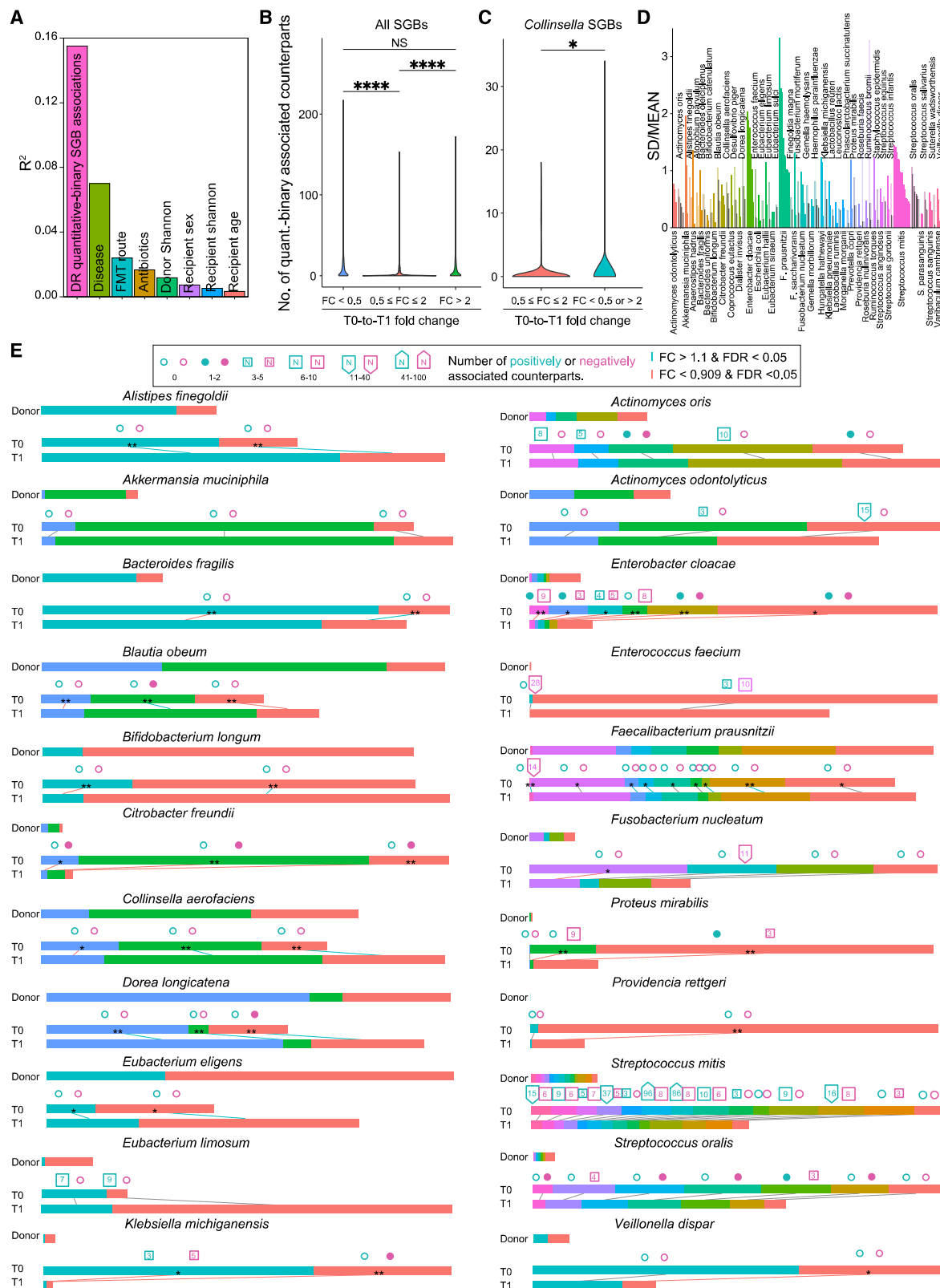
(B) The *Ca. T. transferonalis*-containing subtree encompassing all SGBs in Figure 3A with at least one high-quality (>60% completeness) MAG, with *Faecalibacterium prausnitzii* being included as a phylogenetic reference. A minimum of 1 and a maximum of 10 high-quality MAGs from each SGB are shown.

(C) Principal-coordinate analysis (PCoA) based on genetic distances among MAGs of *Ca. T. transferonalis* ($p < 0.001$, ANOSIM test).

(D) Significant quantitative-binary associations (FDR < 0.05, $\rho > 0.7$ or < -0.7 , Spearman correlation test) of donor *Ca. T. transferonalis* or donor SGB4706 with recipient SGBs. The area of each circle is proportional of its relative abundance in donors (*Ca. T. transferonalis* and SGB4706, at the center) or recipients (all other SGBs). In the network of *Ca. T. transferonalis*, only the 30 most abundant recipient SGBs are labeled.

(E) Numbers of engraftment events (STAR Methods) and donor relative abundances of *Ca. T. transferonalis* or SGB4706. Box edges correspond to lower and upper quartiles, whereas the center line denotes the median, and whiskers extend to 1.5 times the IQR.

(F) KEGG functional profiling of *Ca. T. transferonalis* or SGB4706. The KEGG functions present in <80% and >20% of the samples. The three pathways significantly different between *Ca. T. transferonalis* and SGB4706 (** $p < 0.01$, Wilcoxon rank-sum test) are marked.



(legend on next page)

Another strength of SGB profiling, cemented by referencing to known genomes, is its ability to identify uncharacterized bacteria that potentially play a crucial role but are difficult to culture.^{30,38} Here, we report that SGB4705_Ca. *T. transferonalis*, a microbe in the family of Clostridiaceae, is prevalent across geographic regions, and its engraftment is associated with treatment improvements. Moreover, there is substantial clinical and functional heterogeneity among members in Clostridiaceae, which is depicted by both similarity and incongruence in major clinical and intermicrobial associations between *T. transferonalis* and its close relative SGB4706. Hence, in-depth analyses of members in this subtree, including those yet to be characterized, may uncover microbial genes crucial for FMT, such as those conducive to engraftment. In addition, given their extensive ties to ASD, fine-tuning the methodology of SGB may also help classify the large reservoir of *Collinsella* lineages, where the species-level taxonomy remains insufficiently settled.

Although subspecies-level interactions play a vital role in the engraftment of donor microbes, their effect on subsequent abundance dynamics of introduced members is restrained by multi-strain composition that appears common and relatively stable in gut bacteria. The conserved conspecific landscape may reflect functional differentiation that is needed for a species, or its members, to occupy different niches. The subspecies-level activities over the course of FMT are accompanied by species-level abundance trajectory that typically approaches healthy people, reflecting attenuation of microbiota perturbation at both strain-level (such as the introduction of donor strains) and species-level (such as abundance changes).

STAR★METHODS

Detailed methods are provided in the online version of this paper and include the following:

- KEY RESOURCES TABLE
- RESOURCE AVAILABILITY
 - Lead contact
 - Materials availability
 - Data and code availability
- EXPERIMENTAL MODEL AND SUBJECT DETAILS
 - Recruitment of the in-house ASD cohort
- METHOD DETAILS

- Donor screening and FMT treatment for the ASD patients
- Serum metabolomic analyses for the ASD patients
- Stool metabolomic analyses for the ASD patients
- External metagenomic datasets of FMT
- Building an expanded SGB database
- QUANTIFICATION AND STATISTICAL ANALYSIS
 - SGB profiling of metagenomic samples
 - Analysis of the association between gut microbiome features and clinical indicators or outcome
 - Analysis of DR intermicrobial associations
 - Analysis of mediation effects of metabolic features in-between associated SGBs and ASD indicators
- ADDITIONAL RESOURCES

SUPPLEMENTAL INFORMATION

Supplemental information can be found online at <https://doi.org/10.1016/j.chom.2024.01.013>.

ACKNOWLEDGMENTS

We thank the volunteers and their families for participating in the ASD clinical study and Yue Xu, Shailan Zhou, Chunlian Ma, and anonymous medical staff for performing FMT procedures and collecting clinical information, fecal samples, and blood samples. We thank Lei Yu at Realbio Genomics Institute in metagenomic sequencing. This work was supported by the 3-year action plan of the Shanghai Hospital Development Center (SHDC2022CRS041), the Clinical Research Plan of SHDC (SHDC2020CR1030B and SHDC2020CR4026), the Natural Science Foundation of Shanghai (23ZR1449400), the Clinical Research Plan of SHDC (SHDC2020CR1030B and SHDC2022CRS041), the Scientific and Innovative Action Plan of Shanghai (21Y11908300 and 22DZ2203700), the Ministry of Science and Technology of P.R. China (2022YFA1304100), the Special Development Fund of Zhangjiang National Independent Innovation Demonstration Zone (ZJ2022-ZD005), and the Project of Top Priority Research Center Construction (2023ZZ02007). S.Z. is supported by the National Natural Science Foundation of China (82100677).

AUTHOR CONTRIBUTIONS

H.Q. led the project. Q.X., Q.C., and C.W. conceptualized the study. N.L. established the procedure for donor screening and FMT therapy. C.W. led SGB-based metagenomic analyses. Q.X., Q.C., C.W., J.X., and C.Y. wrote the manuscript. C.Y., H.T., S.Z., L.L., D.Z., X.L., L.W., J.C., Z.L., and J.L. performed FMT treatment, collected stool and blood samples, and documented clinical information. J.X., X.C., N.Z., Y.G., and Q.Y. performed data compilation, bioinformatic analyses, and graphic editing. R.Y., F.Y., and N.Q. assisted

Figure 6. Influences of subspecies-level interactions on donor SGB engraftment and post-FMT composition changes of closely related SGBs

- (A) Effect size of major clinical and microbiome factors on engraftment of donor SGBs.
- (B) Comparison of quantitative-binary-associated SGB numbers between different T0-to-T1 fold change ranges of SGBs in recipients of the 31 datasets (* $p < 0.05$, **** $p < 1 \times 10^{-15}$, Wilcoxon rank-sum test).
- (C) Comparison of quantitative-binary-associated SGB numbers between different T0-to-T1 fold change ranges of *Collinsella* SGBs in recipients of the 31 datasets. There are only 2 *Collinsella* SGBs in T0-to-T1 fold change ranges of <0.5 , as opposed to 238 and 105 SGBs in fold change ranges of 0.5–2 and >2 , thus the “ <0.5 ” and “ >2 ” ranges are merged (* $p < 0.05$, Wilcoxon rank-sum test).
- (D) Standard error normalized by the average relative abundance of constituent SGBs of various bacteria. The standard error results are based on non-zero relative abundance values of each SGB in each participant. SGBs of a same species are in an identical color; bacteria are alternatively labeled at the bottom or top and colored in 100% or 40% opacity, respectively, to avoid overcrowding.
- (E) SGB compositions and association size (number of quantitative-quantitative-associated SGBs, $FDR < 0.1$, Wilcoxon rank-sum test based on relative abundance) of various multi-SGB bacteria. The presented bacteria are representative of over 70 multi-SGB species. In each bacterium, the same SGB is represented by an identical color in donor, T0-recipient, and T1-recipient. Significant changes between T0-recipient and T1-recipient are marked (* $FDR < 0.05$, ** $FDR < 0.01$, Wilcoxon rank-sum test). The cutoff of average relative abundance in T0-recipient and T1-recipient of an SGB is 1×10^{-7} . In each species, the relative abundance values are normalized by the largest combined abundance value among donor, T0-recipient, and T1-recipient. The number of associated lineages is marked for each intra-species SGB.

with FMT treatment and metagenomic sequencing. All authors read the manuscript and provided valuable suggestions.

DECLARATION OF INTERESTS

The authors declare no conflict of interests.

Received: September 19, 2023

Revised: December 8, 2023

Accepted: January 25, 2024

Published: February 16, 2024

REFERENCES

- Fan, Y., and Pedersen, O. (2021). Gut microbiota in human metabolic health and disease. *Nat. Rev. Microbiol.* **19**, 55–71.
- Hanssen, N.M.J., de Vos, W.M., and Nieuwdorp, M. (2021). Fecal microbiota transplantation in human metabolic diseases: from a murky past to a bright future? *Cell Metab.* **33**, 1098–1110.
- Podlesny, D., Durdevic, M., Paramsothy, S., Kaakoush, N.O., Högenauer, C., Gorkiewicz, G., Walter, J., and Fricke, W.F. (2022). Identification of clinical and ecological determinants of strain engraftment after fecal microbiota transplantation using metagenomics. *Cell Rep. Med.* **3**, 100711.
- Schmidt, T.S.B., Li, S.S., Maistrenko, O.M., Akanni, W., Coelho, L.P., Dolai, S., Fullam, A., Glazek, A.M., Hercog, R., Herrema, H., et al. (2022). Drivers and determinants of strain dynamics following fecal microbiota transplantation. *Nat. Med.* **28**, 1902–1912.
- Ianiro, G., Punčochář, M., Karcher, N., Porcari, S., Armanini, F., Asnicar, F., Beghini, F., Blanco-Míguez, A., Cumbo, F., Manghi, P., et al. (2022). Variability of strain engraftment and predictability of microbiome composition after fecal microbiota transplantation across different diseases. *Nat. Med.* **28**, 1913–1923.
- Morais, L.H., Schreiber, H.L., and Mazmanian, S.K. (2021). The gut microbiota–brain axis in behaviour and brain disorders. *Nat. Rev. Microbiol.* **19**, 241–255.
- Vendrik, K.E.W., Ooijsvaar, R.E., de Jong, P.R.C., Laman, J.D., van Oosten, B.W., van Hilten, J.J., Ducarmon, Q.R., Keller, J.J., Kuijper, E.J., and Contarino, M.F. (2020). Fecal microbiota transplantation in neurological disorders. *Front. Cell. Infect. Microbiol.* **10**, 98.
- Yang, Y., Tian, J., and Yang, B. (2018). Targeting gut microbiome: A novel and potential therapy for autism. *Life Sci.* **194**, 111–119.
- Yuen, R.K., Thiruvahindrapuram, B., Merico, D., Walker, S., Tammimies, K., Hoang, N., Chrysler, C., Nalpathamkalam, T., Pellicchia, G., Liu, Y., et al. (2015). Whole-genome sequencing of quartet families with autism spectrum disorder. *Nat. Med.* **21**, 185–191.
- Kim, S., Kim, H., Yim, Y.S., Ha, S., Atarashi, K., Tan, T.G., Longman, R.S., Honda, K., Littman, D.R., Choi, G.B., and Huh, J.R. (2017). Maternal gut bacteria promote neurodevelopmental abnormalities in mouse offspring. *Nature* **549**, 528–532.
- Willsey, H.R., Willsey, A.J., Wang, B., and State, M.W. (2022). Genomics, convergent neuroscience and progress in understanding autism spectrum disorder. *Nat. Rev. Neurosci.* **23**, 323–341.
- Qiu, S., Lu, Y., Li, Y., Shi, J., Cui, H., Gu, Y., Li, Y., Zhong, W., Zhu, X., Liu, Y., et al. (2020). Prevalence of autism spectrum disorder in Asia: A systematic review and meta-analysis. *Psychiatry Res.* **284**, 112679.
- Knopf, A. (2020). Autism prevalence increases from 1 in 60 to 1 in 54: CDC. *Brown Univ. Child Adolesc. Psychopharm. Update* **22**, 6–7.
- Javadfar, Z., Abdollahzad, H., Moludi, J., Rezaeian, S., Amirian, H., Foroughi, A.A., Nachvak, S.M., Goharmehr, N., and Mostafai, R. (2020). Effects of vitamin D supplementation on core symptoms, serum serotonin, and interleukin-6 in children with autism spectrum disorders: A randomized clinical trial. *Nutrition* **79–80**, 110986.
- Wood, J.J., Kendall, P.C., Wood, K.S., Kerns, C.M., Seltzer, M., Small, B.J., Lewin, A.B., and Storch, E.A. (2020). Cognitive behavioral treatments for anxiety in children with autism spectrum disorder: a randomized clinical trial. *JAMA Psychiatry* **77**, 474–483.
- Vargason, T., McGuinness, D.L., and Hahn, J. (2019). Gastrointestinal symptoms and oral antibiotic use in children with autism spectrum disorder: retrospective analysis of a privately insured U.S. population. *J. Autism Dev. Disord.* **49**, 647–659.
- Davies, C., Mishra, D., Eshraghi, R.S., Mittal, J., Sinha, R., Bulut, E., Mittal, R., and Eshraghi, A.A. (2021). Altering the gut microbiome to potentially modulate behavioral manifestations in autism spectrum disorders: A systematic review. *Neurosci. Biobehav. Rev.* **128**, 549–557.
- Parracho, H.M., Bingham, M.O., Gibson, G.R., and McCartney, A.L. (2005). Differences between the gut microflora of children with autistic spectrum disorders and that of healthy children. *J. Med. Microbiol.* **54**, 987–991.
- Wan, Y., Zuo, T., Xu, Z., Zhang, F., Zhan, H., Chan, D., Leung, T.F., Yeoh, Y.K., Chan, F.K.L., Chan, R., and Ng, S.C. (2022). Underdevelopment of the gut microbiota and bacteria species as non-invasive markers of prediction in children with autism spectrum disorder. *Gut* **71**, 910–918.
- Vernocchi, P., Ristori, M.V., Guerrera, S., Guarrasi, V., Conte, F., Russo, A., Lupi, E., Albitar-Nehme, S., Gardini, S., Paci, P., et al. (2022). Gut microbiota ecology and inferred functions in children with ASD compared to neurotypical subjects. *Front. Microbiol.* **13**, 871086.
- Buffington, S.A., Di Prisco, G.V., Auchtung, T.A., Ajami, N.J., Petrosino, J.F., and Costa-Mattioli, M. (2016). Microbial reconstitution reverses maternal diet-induced social and synaptic deficits in offspring. *Cell* **165**, 1762–1775.
- Sgritta, M., Dooling, S.W., Buffington, S.A., Momin, E.N., Francis, M.B., Britton, R.A., and Costa-Mattioli, M. (2019). Mechanisms underlying microbial-mediated changes in social behavior in mouse models of autism spectrum disorder. *Neuron* **101**, 246–259.e6.
- Kang, D.W., Adams, J.B., Gregory, A.C., Borody, T., Chittick, L., Fasano, A., Khoruts, A., Geis, E., Maldonado, J., McDonough-Means, S., et al. (2017). Microbiota Transfer Therapy alters gut ecosystem and improves gastrointestinal and autism symptoms: an open-label study. *Microbiome* **5**, 10.
- Li, N., Chen, H., Cheng, Y., Xu, F., Ruan, G., Ying, S., Tang, W., Chen, L., Chen, M., Lv, L., et al. (2021). Fecal microbiota transplantation relieves gastrointestinal and autism symptoms by improving the gut microbiota in an open-label study. *Front. Cell. Infect. Microbiol.* **11**, 759435.
- Nirmalkar, K., Qureshi, F., Kang, D.W., Hahn, J., Adams, J.B., and Krajmalnik-Brown, R. (2022). Shotgun metagenomics study suggests alteration in sulfur metabolism and oxidative stress in children with autism and improvement after microbiota transfer therapy. *Int. J. Mol. Sci.* **23**, 13481.
- Ahern, P.P., Faith, J.J., and Gordon, J.I. (2014). Mining the human gut microbiota for effector strains that shape the immune system. *Immunity* **40**, 815–823.
- Zhao, S., Lieberman, T.D., Poyet, M., Kauffman, K.M., Gibbons, S.M., Groussin, M., Xavier, R.J., and Alm, E.J. (2019). Adaptive evolution within gut microbiomes of healthy people. *Cell Host Microbe* **25**, 656–667.e8.
- Wilson, B.C., Vatanen, T., Jayasinghe, T.N., Leong, K.S.W., Derraik, J.G.B., Albert, B.B., Chiavaroli, V., Svirskis, D.M., Beck, K.L., Conlon, C.A., et al. (2021). Strain engraftment competition and functional augmentation in a multi-donor fecal microbiota transplantation trial for obesity. *Microbiome* **9**, 107.
- Schloissnig, S., Arumugam, M., Sunagawa, S., Mitreva, M., Tap, J., Zhu, A., Waller, A., Mende, D.R., Kultima, J.R., Martin, J., et al. (2013). Genomic variation landscape of the human gut microbiome. *Nature* **493**, 45–50.
- Pasolli, E., Asnicar, F., Manara, S., Zolfo, M., Karcher, N., Armanini, F., Beghini, F., Manghi, P., Tett, A., Ghensi, P., et al. (2019). Extensive unexplored human microbiome diversity revealed by over 150,000 genomes from metagenomes spanning age, geography, and lifestyle. *Cell* **176**, 649–662.e20.

31. Kurkjian, H.M., Akbari, M.J., and Momeni, B. (2021). The impact of interactions on invasion and colonization resistance in microbial communities. *PLoS Comput. Biol.* **17**, e1008643.
32. Ianaro, G., Rossi, E., Thomas, A.M., Schinzari, G., Masucci, L., Quaranta, G., Settanni, C.R., Lopetuso, L.R., Armanini, F., Blanco-Míguez, A., et al. (2020). Faecal microbiota transplantation for the treatment of diarrhoea induced by tyrosine-kinase inhibitors in patients with metastatic renal cell carcinoma. *Nat. Commun.* **11**, 4333.
33. Kong, L., Lloyd-Price, J., Vatanen, T., Seksik, P., Beaugerie, L., Simon, T., Vlamakis, H., Sokol, H., and Xavier, R.J. (2020). Linking strain engraftment in fecal microbiota transplantation with maintenance of remission in Crohn's disease. *Gastroenterology* **159**, 2193–2202.e5.
34. Li, S.S., Zhu, A., Benes, V., Costea, P.I., Hercog, R., Hildebrand, F., Huerta-Cepas, J., Nieuwdorp, M., Salojärvi, J., Voigt, A.Y., et al. (2016). Durable coexistence of donor and recipient strains after fecal microbiota transplantation. *Science* **352**, 586–589.
35. Podlesny, D., Arze, C., Dörner, E., Verma, S., Dutta, S., Walter, J., and Fricke, W.F. (2022). Metagenomic strain detection with SameStr: identification of a persisting core gut microbiota transferable by fecal transplantation. *Microbiome* **10**, 53.
36. Smillie, C.S., Sauk, J., Gevers, D., Friedman, J., Sung, J., Youngster, I., Hohmann, E.L., Staley, C., Khoruts, A., Sadowsky, M.J., et al. (2018). Strain tracking reveals the determinants of bacterial engraftment in the human gut following fecal microbiota transplantation. *Cell Host Microbe* **23**, 229–240.e5.
37. Nielsen, H.B., Almeida, M., Juncker, A.S., Rasmussen, S., Li, J., Sunagawa, S., Plichta, D.R., Gautier, L., Pedersen, A.G., Le Chatelier, E., et al. (2014). Identification and assembly of genomes and genetic elements in complex metagenomic samples without using reference genomes. *Nat. Biotechnol.* **32**, 822–828.
38. Blanco-Míguez, A., Beghini, F., Cumbo, F., McIver, L.J., Thompson, K.N., Zolfo, M., Manghi, P., Dubois, L., Huang, K.D., Thomas, A.M., et al. (2023). Extending and improving metagenomic taxonomic profiling with uncharacterized species using MetaPhlAn 4. *Nat. Biotechnol.* **41**, 1633–1644.
39. Zhang, S., Chen, Q., Kelly, C.R., Kassam, Z., Qin, H., Li, N., Shanghai Tongji FMT Working Group, Tian, H., Yang, B., Zhao, D., et al. (2022). Donor screening for fecal microbiota transplantation in China: evaluation of 8483 candidates. *Gastroenterology* **162**, 966–968.e3.
40. Tian, H., Zhang, S., Qin, H., Li, N., and Chen, Q. (2022). Long-term safety of faecal microbiota transplantation for gastrointestinal diseases in China. *Lancet Gastroenterol. Hepatol.* **7**, 702–703.
41. Stewart, C.J., Ajami, N.J., O'Brien, J.L., Hutchinson, D.S., Smith, D.P., Wong, M.C., Ross, M.C., Lloyd, R.E., Doddapaneni, H., Metcalf, G.A., et al. (2018). Temporal development of the gut microbiome in early childhood from the TEDDY study. *Nature* **562**, 583–588.
42. Morgan, X.C., Tickle, T.L., Sokol, H., Gevers, D., Devaney, K.L., Ward, D.V., Reyes, J.A., Shah, S.A., LeLeiko, N., Snapper, S.B., et al. (2012). Dysfunction of the intestinal microbiome in inflammatory bowel disease and treatment. *Genome Biol.* **13**, R79.
43. Ding, X., Xu, Y., Zhang, X., Zhang, L., Duan, G., Song, C., Li, Z., Yang, Y., Wang, Y., Wang, X., and Zhu, C. (2020). Gut microbiota changes in patients with autism spectrum disorders. *J. Psychiatr. Res.* **729**, 149–159.
44. Strati, F., Cavallieri, D., Albanese, D., De Felice, C., Donati, C., Hayek, J., Jousson, O., Leoncini, S., Renzi, D., Calabrò, A., and De Filippo, C. (2017). New evidences on the altered gut microbiota in autism spectrum disorders. *Microbiome* **5**, 24.
45. Chu, J.H., Bian, F., Yan, R.Y., Li, Y.L., Cui, Y.H., and Li, Y. (2022). Comparison of diagnostic validity of two autism rating scales for suspected autism in a large Chinese sample. *World J. Clin. Cases* **10**, 1206–1217.
46. Rellini, E., Tortolani, D., Trillo, S., Carbone, S., and Montecchi, F. (2004). Childhood Autism Rating Scale (CARS) and Autism Behavior Checklist (ABC) correspondence and conflicts with DSM-IV criteria in diagnosis of autism. *J. Autism Dev. Disord.* **34**, 703–708.
47. Truong, D.T., Tett, A., Pasolli, E., Huttenhower, C., and Segata, N. (2017). Microbial strain-level population structure and genetic diversity from metagenomes. *Genome Res.* **27**, 626–638.
48. Colpaert, E.E., Timmermans, J.P., and Lefebvre, R.A. (2002). Investigation of the potential modulatory effect of biliverdin, carbon monoxide and bilirubin on nitrgic neurotransmission in the pig gastric fundus. *Eur. J. Pharmacol.* **457**, 177–186.
49. Currais, A., Huang, L., Goldberg, J., Petrascheck, M., Ates, G., Pinto-Duarte, A., Shokhirev, M.N., Schubert, D., and Maher, P. (2019). Elevating acetyl-CoA levels reduces aspects of brain aging. *Elife* **8**, e47866.
50. Siggins, G.R., Gruol, D.L., Padjen, A.L., and Formans, D.S. (1977). Purine and pyrimidine mononucleotides depolarise neurones of explanted amphibian sympathetic ganglia. *Nature* **270**, 263–265.
51. Wyrembek, P., Negri, R., Kaczor, P., Czyżewska, M., Appendino, G., and Mozrzymas, J.W. (2012). Falcariindol allosterically modulates GABAergic currents in cultured rat hippocampal neurons. *J. Nat. Prod.* **75**, 610–616.
52. McMillin, M., and DeMorrow, S. (2016). Effects of bile acids on neurological function and disease. *FASEB J.* **30**, 3658–3668.
53. Busardó, F.P., Frati, P., Sanzo, M.D., Napoletano, S., Pinchi, E., Zaami, S., and Fineschi, V. (2015). The impact of nandrolone decanoate on the central nervous system. *Curr. Neuropharmacol.* **13**, 122–131.
54. Beaudet, A.L. (2017). Brain carnitine deficiency causes nonsyndromic autism with an extreme male bias: A hypothesis. *BioEssays* **39**, 1700012.
55. Ehehalt, R., Braun, A., Karner, M., Füllekrug, J., and Stremmel, W. (2010). Phosphatidylcholine as a constituent in the colonic mucosal barrier—physiological and clinical relevance. *Biochim. Biophys. Acta* **1801**, 983–993.
56. Tagesson, C., Franzén, L., Dahl, G., and Weström, B. (1985). Lysophosphatidylcholine increases rat ileal permeability to macromolecules. *Gut* **26**, 369–377.
57. Aggarwala, V., Mogno, I., Li, Z., Yang, C., Britton, G.J., Chen-Liaw, A., Mitcham, J., Bongers, G., Gevers, D., Clemente, J.C., et al. (2021). Precise quantification of bacterial strains after fecal microbiota transplantation delineates long-term engraftment and explains outcomes. *Nat. Microbiol.* **6**, 1309–1318.
58. Bar-Yoseph, H., Carasso, S., Shklar, S., Korytny, A., Even Dar, R., Daoud, H., Nassar, R., Maharshak, N., Hussein, K., Geffen, Y., et al. (2021). Oral capsulized fecal microbiota transplantation for eradication of carbapenemase-producing Enterobacteriaceae colonization with a metagenomic perspective. *Clin. Infect. Dis.* **73**, e166–e175.
59. Baruch, E.N., Youngster, I., Ben-Betzalel, G., Ortenberg, R., Lahat, A., Katz, L., Adler, K., Dick-Necula, D., Raskin, S., Bloch, N., et al. (2021). Fecal microbiota transplant promotes response in immunotherapy-refractory melanoma patients. *Science* **371**, 602–609.
60. Damman, C.J., Brittnacher, M.J., Westerhoff, M., Hayden, H.S., Radey, M., Hager, K.R., Marquis, S.R., Miller, S.I., and Zisman, T.L. (2015). Low Level Engraftment and Improvement following a Single Colonoscopic Administration of Fecal Microbiota to Patients with Ulcerative Colitis. *PLoS One* **10**, e0133925.
61. Davar, D., Dzutsev, A.K., McCulloch, J.A., Rodrigues, R.R., Chauvin, J.M., Morrison, R.M., Deblasio, R.N., Menna, C., Ding, Q., Pagliano, O., et al. (2021). Fecal microbiota transplant overcomes resistance to anti-PD-1 therapy in melanoma patients. *Science* **371**, 595–602.
62. Goll, R., Johnsen, P.H., Hjerde, E., Diab, J., Valle, P.C., Hilpusch, F., and Cavanagh, J.P. (2020). Effects of fecal microbiota transplantation in subjects with irritable bowel syndrome are mirrored by changes in gut microbiome. *Gut Microbes* **12**, 1794263.
63. Goloshchapov, O.V., Olekhovich, E.I., Sidorenko, S.V., Moiseev, I.S., Kucher, M.A., Fedorov, D.E., Pavlenko, A.V., Manolov, A.I., Gostev, V.V., Veselovsky, V.A., et al. (2019). Long-term impact of fecal transplantation in healthy volunteers. *BMC Microbiol.* **19**, 312.
64. Hourigan, S.K., Ahn, M., Gibson, K.M., Pérez-Losada, M., Felix, G., Weidner, M., Leibowitz, I., Niederhuber, J.E., Sears, C.L., Crandall,

- K.A., and Oliva-Hemker, M. (2019). Fecal transplant in children with *Clostridioides difficile* gives sustained reduction in antimicrobial resistance and potential pathogen burden. *Open Forum Infect. Dis.* 6, ofz379.
65. Koopen, A.M., Almeida, E.L., Attaye, I., Witjes, J.J., Rampanelli, E., Majait, S., Kemper, M., Levels, J.H.M., Schimmel, A.W.M., Herrema, H., et al. (2021). Effect of fecal microbiota transplantation combined with Mediterranean diet on insulin sensitivity in subjects with metabolic syndrome. *Front. Microbiol.* 12, 662159.
66. Kootte, R.S., Levin, E., Salojärvi, J., Smits, L.P., Hartstra, A.V., Udayappan, S.D., Hermes, G., Bouter, K.E., Koopen, A.M., Holst, J.J., et al. (2017). Improvement of insulin sensitivity after lean donor feces in metabolic syndrome is driven by baseline intestinal microbiota composition. *Cell Metab.* 26, 611–619.e6.
67. Kumar, R., Yi, N., Zhi, D., Eipers, P., Goldsmith, K.T., Dixon, P., Crossman, D.K., Crowley, M.R., Lefkowitz, E.J., Rodriguez, J.M., and Morrow, C.D. (2017). Identification of donor microbe species that colonize and persist long term in the recipient after fecal transplant for recurrent *Clostridium difficile*. *NPJ Biofilms Microbiomes* 3, 12.
68. Lee, S.T.M., Kahn, S.A., Delmont, T.O., Shaiber, A., Esen, Ö.C., Hubert, N.A., Morrison, H.G., Antonopoulos, D.A., Rubin, D.T., and Eren, A.M. (2017). Tracking microbial colonization in fecal microbiota transplantation experiments via genome-resolved metagenomics. *Microbiome* 5, 50.
69. Leo, S., Lazarevic, V., Girard, M., Gaia, N., Schrenzel, J., de Lastours, V., Fantin, B., Bonten, M., Carmeli, Y., Rondinaud, E., et al. (2020). Metagenomic characterization of gut microbiota of carriers of extended-spectrum beta-lactamase or carbapenemase-producing Enterobacteriaceae following treatment with oral antibiotics and fecal microbiota transplantation: results from a multicenter randomized trial. *Microorganisms* 8, 941.
70. Moss, E.L., Falconer, S.B., Tkachenko, E., Wang, M., Systrom, H., Mahabamunuge, J., Relman, D.A., Hohmann, E.L., and Bhatt, A.S. (2017). Long-term taxonomic and functional divergence from donor bacterial strains following fecal microbiota transplantation in immunocompromised patients. *PLoS One* 12, e0182585.
71. Nusbaum, D.J., Sun, F., Ren, J., Zhu, Z., Ramsy, N., Pervolarakis, N., Kunde, S., England, W., Gao, B., Fiehn, O., et al. (2018). Gut microbial and metabolomic profiles after fecal microbiota transplantation in pediatric ulcerative colitis patients. *FEMS Microbiol. Ecol.* 94, fty133.
72. Rossen, N.G., Fuentes, S., van der Spek, M.J., Tijssen, J.G., Hartman, J.H., Duflo, A., Löwenberg, M., van den Brink, G.R., Mathus-Vliegen, E.M., de Vos, W.M., et al. (2015). Findings from a randomized controlled trial of fecal transplantation for patients with ulcerative colitis. *Gastroenterology* 149, 110–118.e4.
73. Singh, R., de Groot, P.F., Geerlings, S.E., Hodiament, C.J., Belzer, C., Berge, I.J.M.T., de Vos, W.M., Bemelman, F.J., and Nieuwdorp, M. (2018). Fecal microbiota transplantation against intestinal colonization by extended spectrum beta-lactamase producing Enterobacteriaceae: a proof of principle study. *BMC Res. Notes* 11, 190.
74. Vaughn, B.P., Vatanen, T., Allegretti, J.R., Bai, A., Xavier, R.J., Korzenik, J., Gevers, D., Ting, A., Robson, S.C., and Moss, A.C. (2016). Increased intestinal microbial diversity following fecal microbiota transplant for active Crohn's disease. *Inflamm. Bowel Dis.* 22, 2182–2190.
75. Verma, S., Dutta, S.K., Firnberg, E., Phillips, L., Vinayek, R., and Nair, P.P. (2021). Identification and engraftment of new bacterial strains by shotgun metagenomic sequence analysis in patients with recurrent *Clostridioides difficile* infection before and after fecal microbiota transplantation and in healthy human subjects. *PLoS One* 16, e0251590.
76. Watson, A.R., Füssel, J., Veseli, I., DeLongchamp, J.Z., Silva, M., Trigodet, F., Lolans, K., Shaiber, A., Fogarty, E., Runde, J.M., et al. (2023). Metabolic independence drives gut microbial colonization and resilience in health and disease. *Genome Biol.* 24, 78.
77. Zhao, H.J., Luo, X., Shi, Y.C., Li, J.F., Pan, F., Ren, R.R., Peng, L.H., Shi, X.Y., Yang, G., Wang, J., et al. (2020). The efficacy of fecal microbiota transplantation for children with Tourette syndrome: A preliminary study. *Front. Psychiatry* 11, 554441.
78. Coyte, K.Z., and Rakoff-Nahoum, S. (2019). Understanding Competition and Cooperation within the Mammalian Gut microbiome. *Curr. Biol.* 29, R538–R544.
79. Kim, C.Y., Lee, M., Yang, S., Kim, K., Yong, D., Kim, H.R., and Lee, I. (2021). Human reference gut microbiome catalog including newly assembled genomes from under-represented Asian metagenomes. *Genome Med.* 13, 134.
80. Yeoh, Y.K., Sun, Y., Ip, L.Y.T., Wang, L., Chan, F.K.L., Miao, Y., and Ng, S.C. (2022). *Prevotella* species in the human gut is primarily comprised of *Prevotella copri*, *Prevotella stercorea* and related lineages. *Sci. Rep.* 12, 9055.
81. Zhu, J., Tian, L., Chen, P., Han, M., Song, L., Tong, X., Sun, X., Yang, F., Lin, Z., Liu, X., et al. (2022). Over 50,000 metagenomically assembled draft genomes for the human oral microbiome reveal new taxa. *Genomics Proteomics Bioinformatics* 20, 246–259.
82. Lopez-Siles, M., Duncan, S.H., Garcia-Gil, L.J., and Martinez-Medina, M. (2017). *Faecalibacterium prausnitzii*: from microbiology to diagnostics and prognostics. *ISME J.* 11, 841–852.
83. Valles-Colomer, M., Falony, G., Darzi, Y., Tigchelaar, E.F., Wang, J., Tito, R.Y., Schiweck, C., Kurilshikov, A., Joossens, M., Wijmenga, C., et al. (2019). The neuroactive potential of the human gut microbiota in quality of life and depression. *Nat. Microbiol.* 4, 623–632.
84. Derrien, M., Turroni, F., Ventura, M., and van Sinderen, D. (2022). Insights into endogenous *Bifidobacterium* species in the human gut microbiota during adulthood. *Trends Microbiol.* 30, 940–947.
85. Asnicar, F., Weingart, G., Tickle, T.L., Huttenhower, C., and Segata, N. (2015). Compact graphical representation of phylogenetic data and metadata with GraPhlAn. *PeerJ* 18, e1029.
86. Cantalapiedra, C.P., Hernández-Plaza, A., Letunic, I., Bork, P., and Huerta-Cepas, J. (2021). eggNOG-mapper v2: Functional Annotation, Orthology Assignments, and Domain Prediction at the Metagenomic Scale. *Mol. Biol. Evol.* 38, 5825–5829. <https://doi.org/10.1093/molbev/msab293>.
87. Asnicar, F., Thomas, A. M., Beghini, F., Mengoni, C., Manara, S., Manghi, P., Zhu, Q., Bolzan, M., Cumbo, F., May, U., et al. (2020). Precise phylogenetic analysis of microbial isolates and genomes from metagenomes using PhyloPhlAn 3.0. *Nat. Commun.* 11, 2500. <https://doi.org/10.1038/s41467-020-16366-7>.
88. Langmead, B., and Salzberg, S.L. (2012). Fast gapped-read alignment with Bowtie 2. *Nat. Methods.* 9, 357–359. <https://doi.org/10.1038/nmeth.1923>.
89. Ondov, B.D., Treangen, T.J., Melsted, P., Mallonee, A.B., Bergman, N.H., Koren, S., and Phillippy, A.M. (2016). Mash: fast genome and metagenome distance estimation using MinHash. *Genome Biol.* 17, 132. <https://doi.org/10.1186/s13059-016-0997-x>.
90. Nurk, S., Meleshko, D., Korobeynikov, A., and Pevzner, P.A. (2017). metaSPAdes: a new versatile metagenomic assembler. *Genome Res* 27, 824–834. <https://doi.org/10.1101/gr.213959.116>.
91. Seemann, T. (2014). Prokka: rapid prokaryotic genome annotation. *Bioinformatics (Oxford, England)* 30, 2068–2069. <https://doi.org/10.1093/bioinformatics/btu153>.
92. Buchfink, B., Reuter, K., and Drost, H.-G. (2021). Sensitive protein alignments at tree-of-life scale using DIAMOND. *Nat Methods* 18, 366–368. <https://doi.org/10.1038/s41592-021-01101-x>.
93. Stamatakis, A. (2014). RAxML version 8: a tool for phylogenetic analysis and post-analysis of large phylogenies. *Bioinformatics (Oxford, England)* 30, 1312–1313. <https://doi.org/10.1093/bioinformatics/btu033>.
94. Parks, D.H., Imelfort, M., Skennerton, C.T., Hugenholtz, P., and Tyson, G.W. (2015). CheckM: assessing the quality of microbial genomes recovered from isolates, single cells, and metagenomes. *Genome Res* 25, 1043–1055. <https://doi.org/10.1101/gr.186072.114>.

95. Kang, D.D., Li, F., Kirton, E., Thomas, A., Egan, R., An, H., and Wang, Z. (2019). MetaBAT 2: an adaptive binning algorithm for robust and efficient genome reconstruction from metagenome assemblies. *PeerJ* 7, e7359. <https://doi.org/10.7717/peerj.7359>.
96. Chambers, M.C., Maclean, B., Burke, R., Amodei, D., Ruderman, D.L., Neumann, S., Gatto, L., Fischer, B., Pratt, B., Egertson, J., et al. (2012). A cross-platform toolkit for mass spectrometry and proteomics. *Nat Biotechnol* 30, 918–920. <https://doi.org/10.1038/nbt.2377>.
97. B. MacLean, D.M. Tomazela, N. Shulman, M. Chambers, G.L. Finney, B. Frewen, R. Kern, D.L. Tabb, D.C. Liebler, and M.J. MacCoss, eds. (2010). 26, 966–968. <https://doi.org/10.1093/bioinformatics/btq054>.
98. Mallick, H., Rahnavard, A., McIver, L.J., Ma, S., Zhang, Y., Nguyen, L.H., Tickle, T.L., Weingart, G., Ren, B., Schwager, E.H., et al. (2021). Multivariable association discovery in population-scale meta-omics studies. *PLoS Comput. Biol.* 17, e1009442. <https://doi.org/10.1371/journal.pcbi.1009442>.
99. Olm, M.R., Crits-Christoph, A., Bouma-Gregson, K., Firek, B.A., Morowitz, M.J., and Banfield, J.F. (2021). inStrain profiles population microdiversity from metagenomic data and sensitively detects shared microbial strains. *Nat. Biotechnol.* 39, 727–736. <https://doi.org/10.1038/s41587-020-00797-0>.
100. Parenteral and Enteral Nutrition Branch of Chinese Medical Association; Enhanced Recovery After Surgery Branch of China International Health Care Promotion and Exchange Association; China Microecological Treatment Innovation Alliance; Microecology Committee of Shanghai Preventive Medicine Association (2020). [Chinese experts consensus on standardized methodology and clinical application of fecal microbiota transplantation]. *Zhonghua Wei Chang Wai Ke Za Zhi* 23, 5–13.
101. Huerta-Cepas, J., Szklarczyk, D., Forslund, K., Cook, H., Heller, D., Walter, M.C., Rattei, T., Mende, D.R., Sunagawa, S., Kuhn, M., et al. (2016). eggNOG 4.5: a hierarchical orthology framework with improved functional annotations for eukaryotic, prokaryotic and viral sequences. *Nucleic Acids Res.* 44, D286–D293.

STAR★METHODS

KEY RESOURCES TABLE

REAGENT or RESOURCE	SOURCE	IDENTIFIER
Biological samples		
Fecal samples (ASD cohort)	This paper	IRB# SHSY-IEC-5.0/21k8/P01
Serum samples (ASD cohort)	This paper	IRB# SHSY-IEC-5.0/21k8/P01
Critical commercial assays		
QIAamp PowerFecal DNA Kit	Qiagen	Cat# 12830-50
NEXTflex™ Rapid DNA-Seq Kit	Bioo Scientific	Cat# NOVA-5144-08
UHPLC system	Thermo Fisher Scientific	Vanquish
QE HFX mass spectrometer	Thermo Fisher Scientific	Q Exactive HFX
Deposited data		
Raw sequencing data (ASD cohort)	This paper	NCBI-SRA BioProject: PRJNA1010504
Software and Algorithms		
GraPhlAn (version 1.1.3)	Asnicar et al., 2015 ⁸⁵	https://github.com/biobakery/graphlan
EggNOG mapper (version 2.1.10)	Cantalapiedra et al., 2021 ⁸⁶	https://github.com/eggnogetdb/eggnoget-mapper/releases
PhyloPhlAn (version 3.0.67)	Asnicar et al., 2020 ⁸⁷	https://github.com/biobakery/phylophlan/releases
StrainPhlAn (version 4.0.3)	Blanco-Míguez et al. ³⁸	https://github.com/biobakery/MetaPhlAn/wiki/StrainPhlAn-4
MetaPhlAn4 (version 4.0.3)	Blanco-Míguez et al. ³⁸	https://github.com/biobakery/MetaPhlAn/wiki/MetaPhlAn-4
bowtie2 (version 2.4.3)	Langmead and Salzberg, 2012 ⁸⁸	https://sourceforge.net/projects/bowtie-bio/files/bowtie2/
mash (version 2.0.0)	Ondov et al., 2016 ⁸⁹	https://github.com/marbl/Mash/releases
metaSPAdes (version 3.15.4)	Nurk et al., 2017 ⁹⁰	https://github.com/ablab/spades/releases
prokka (version 1.14.6)	Seeman, 2014 ⁹¹	https://github.com/tseemann/prokka/releases
Diamond (version 2.1.3.157)	Buchfink et al., 2021 ⁹²	https://github.com/bbuchfink/diamond/
RAXML (version 8.2.12)	Stamatakis, 2014 ⁹³	https://github.com/stamatak/standard-RAXML
CheckM (version 1.0.7)	Parks et al., 2015 ⁹⁴	https://github.com/ECogenomics/CheckM/releases
MetaBAT2 (version 2.12.1)	Kang et al., 2019 ⁹⁵	https://bitbucket.org/berkeleylab/metabat
ProteoWizard (version 3)	Chambers et al., 2012 ⁹⁶	https://proteowizard.sourceforge.io/download.html
Skyline (version 20.2)	Maclean et al., 2010 ⁹⁷	https://skyline.ms/project/home/begin.view?/
MaAsLin (version 2.0)	Mallick et al., 2021 ⁹⁸	https://github.com/biobakery/biobakery/wiki/maaslin2
hmmer (version 3.1b1)	N/A	http://hmmer.org/download.html
inStrain (version 1.5.4)	Olm et al., 2021 ⁹⁹	https://github.com/MrOlm/inStrain/tree/master
Other		
LIVE/DEAD™ BacLight™ Bacterial Viability and Counting Kit	Thermo Fisher Scientific	Cat# L34856

RESOURCE AVAILABILITY

Lead contact

Further information and requests should be directed to the lead contact, Qian Xu (uncqxu@gmail.com).

Materials availability

This study did not generate new unique reagents.

Data and code availability

- The serum and stool metabolomic raw data of the in-house ASD cohort are in [Table S1](#). The metagenomic sequencing data of the in-house ASD cohort are deposited in the National Center for Biotechnology Information Sequence Read Archive database under accession number PRJNA1010504. The included metagenomic datasets and their sequencing data statistics are summarized in [Table S2](#).

- No new code was generated in this study.
- Any additional information required to reanalyze the data reported in this work paper is available from the [lead contact](#) upon request.

EXPERIMENTAL MODEL AND SUBJECT DETAILS

Recruitment of the in-house ASD cohort

Between February 2019 and February 2021, 68 consecutive pediatric patients diagnosed with autism spectrum disorder (ASD), who were 2–13 years old, were screened for eligibility to enter the prospective FMT-based study that was registered at the Chinese Clinical Trial Registry. The inclusion criteria were the follows: i). meeting the diagnostic criteria of ASD in the Diagnostic and Statistical Manual of Mental Disorders (DSM-5-TR) issued by the American Psychiatric Association; ii). having a gastrointestinal (GI) comorbidity of constipation, diarrhea, bloating, abdominal pain or food allergy/intolerance for at least 6 months. The exclusion criteria were the follows: i). Rett syndrome; ii). a history of brain conditions including traumatic brain injury, cerebral palsy or encephalitis; iii). a history of other mental disorders; iv). a history of GI diseases including Hirschsprung's disease, intestinal obstruction or intussusception; v). a history of pathological intestinal inflammatory conditions such as inflammatory bowel disease (IBD); vi). a history of severe obesity or severe malnutrition; vii). administration of probiotics, antibiotics or other agents likely affecting gut microbes 3 months before, and during, the 6-month study; viii). having received FMT 12 months before the recruitment; ix). difficulty in swallowing #3 FMT capsules. As a consequence, 29 ASD patients, along with 36 age/sex-matched healthy controls, were recruited. Informed consent was obtained from the guardians of all participants. Donor screening and preparation of FMT capsules were performed according to Chinese Expert Consensus FMT guideline.^{39,100} This study was performed in compliance of the Declaration of Helsinki. The research protocol was approved by the Ethics Committee of the Tenth People's Hospital, Tongji University School of Medicine.

METHOD DETAILS

Donor screening and FMT treatment for the ASD patients

Donors were enrolled after two rounds of screening, referred as Donor Evaluation (comprising lifestyle and medical history questionnaires and basic medical examinations) and Donor Selection (comprising medical risk questionnaires and laboratory tests on stool, blood, and urine samples) to minimize health risks.³⁹ This included extensive stool, blood and urine tests to screen for the presence of bacterial, viral, fungal, and protozoan pathogens before or after stool processing, which involved plate culture, serology, polymerase chain reaction, and microscopy.^{39,100} As a consequence, seven donors aged between 24 and 28 were selected (Figure 1). The stool samples from healthy donors were percolated, centrifuged and lyophilized, before the resulting powder was transferred into acid-resistant hydroxypropyl methylcellulose capsules, which were refrigerated at -80°C. As a quality control, live bacteria per capsule had a minimal concentration of 5.0×10^9 bacteria/g and accounted for more than 70% of total bacterial cells, assessed using flow cytometry after staining capsule content with LIVE/DEAD BacLight Bacterial Viability Kit (Thermo Fisher Scientific).

All patients received a 4-month FMT regimen of 4-session, oral administration of microbiota capsules (Figure 1), which involved no antibiotic pretreatment or bowel cleansing before the intervention. In each monthly session, a patient first received clinical assessments of autism and gastrointestinal symptoms on indicators listed below, followed by FMT therapy beginning on the same or next day, which involved two oral administrations daily, each with 2 FMT capsules, for 12 consecutive days; the aggregated monthly administration of 48 capsules contained bacteria equivalent to that of 200 g fresh stool. 1 h before and after taking capsules, food and drink were not permitted. Approximately two weeks after the entire therapy, a follow-up visit was paid to each patient for final evaluation. The clinical assessments were based on Autism Behavior Checklist (ABC), Childhood Autism Rating Scale (CARS), Bristol Stool Form Scale (BSFS), and Childhood Autism Rating Scale (GSRS).

Serum metabolomic analyses for the ASD patients

Metabolomic analyses were performed with the assistance from Shanghai Biotree Biotech. Blood samples were drawn from participants in the morning after overnight fasting and at least 24 h of alcoholic abstinence, which were centrifuged at 3,000 rpm for 5 min to generate sera. Aliquots in 3×1.5 ml parafilm-sealed microcentrifuge tubes were stored in a -80 °C freezer. For untargeted metabolomic analyses, 50 µL sample was transferred to an Eppendorf tube and was supplemented with 200 µL extract solution (acetonitrile: methanol = 1: 1, containing isotopically labeled internal standard mixture). The mixture was vortexed for 30 s, sonicated for 10 min in ice-water bath, and incubated for 1 h at -40°C to facilitate protein precipitation. The samples were centrifuged at 12,000 rpm (RCF = 13,800 g, R = 8.6 cm) and at 4°C for 15 min, and the resulting supernatant was transferred to a fresh glass vial for analysis. The quality control (QC) sample was prepared by mixing an equal volume of the supernatants from all of the samples. LC-MS/MS analyses were performed by using an UHPLC system (Vanquish, Thermo Fisher Scientific) with a UPLC BEH Amide column (2.1 mm × 100 mm, 1.7 µm) coupled to Q Exactive HFX mass spectrometer (Orbitrap MS, Thermo Fisher Scientific). The mobile phase consisted of 25 mmol/L ammonium acetate and 25 mmol/L ammonia hydroxide in water (pH = 9.75) (A) and acetonitrile (B). The auto-sampler temperature was 4°C, and the injection volume was 3 µL.

The QE HFX mass spectrometer was used for its ability to acquire MS/MS spectra on information-dependent acquisition (IDA) mode in the control of the acquisition software (Xcalibur, Thermo Fisher Scientific). In this mode, the acquisition software

continuously evaluates the full scan MS spectrum. The ESI source conditions were set as follows: sheath gas flow rate of 30 Arb, Aux gas flow rate of 25 Arb, capillary temperature of 350°C, full MS resolution of 60000, MS/MS resolution of 7500, collision energy of 10/30/60 in NCE mode, and spray Voltage of 3.6 kV or -3.2 kV, respectively. The raw data were converted to the mzXML format using ProteoWizard and were processed with an in-house XCMS-based algorithm in R scripts for peak detection, extraction, alignment, and integration. A custom MS2 database (BiotreeDB) was referenced for metabolite annotation, with an annotation cutoff at 0.3.

For targeted analysis of serum neurotransmitters, 20 μ L of each sample was transferred to an Eppendorf tube and was supplemented with 80 μ L extraction solvent (acetonitrile with 0.1% (v/v) formic acid, precooled at -20°C). The samples were vortexed for 30 s and sonicated for 15 min in ice-water bath, followed by incubation at -40°C overnight and centrifugation at 12,000 rpm and at 4°C for 15 min. 80 μ L supernatant was transferred to an Eppendorf tube, supplemented with 40 μ L 100 mM sodium carbonate and 40 μ L 2% benzoyl chloride acetonitrile, and was incubated at room temperature for 30 min. The samples were supplemented with 10 μ L internal standard and centrifuged at 12000 rpm and at 4°C for 15 min. 40 μ L supernatant was mixed with 20 μ L H₂O and transferred to an auto-sampler vial for UHPLC-MS/MS analysis. The UHPLC separation was carried out using an ExionLC System, equipped with a Waters ACQUITY UPLC HSS T3 (100 \times 2.1 mm, 1.8 μ m). The mobile phase A comprised 0.1% formic acid and 1mM ammonium formate in water, and the mobile phase B was acetonitrile. The column temperature was set at 40°C; the auto-sampler temperature was set at 4°C; the injection volume was 1 μ L. AB Sciex QTrap 6500+ mass spectrometer was applied for assay development. Typical ion source parameters were: IonSpray Voltage: +5000V, Curtain Gas: 35 psi, Temperature: 400°C, Ion Source Gas 1: 60 psi, Ion Source Gas 2: 60 psi. Skyline Software was employed for MRM data processing.

Stool metabolomic analyses for the ASD patients

Stool samples were air dried and supplemented with extract buffer (methanol: acetonitrile: water = 2:2:1 (v/v/v), containing isotope labeled internal standard mixture) at a ratio of 25 mg dry sample per 500 μ L extract buffer. The mixtures were subjected to 3 cycles of 4-min homogenization and 5-min sonication in ice-water bath and were incubated for 1 h at -40°C and centrifuged at 12,000 rpm for 15 min at 4°C. The resulting supernatant was transferred to a fresh glass vial for analysis. The quality control (QC) sample was prepared by mixing an equal aliquot of the supernatants from all of the samples. LC-MS/MS analyses were performed using an UHPLC system (Vanquish, Thermo Fisher Scientific) with a UPLC BEH Amide column (2.1 mm \times 100 mm, 1.7 μ m) coupled to Q Exactive HFX mass spectrometer (Orbitrap MS, Thermo Fisher Scientific). The mobile phase consisted of 25 mmol/L ammonium acetate and 25 ammonia hydroxide in water (pH = 9.75) (A) and acetonitrile (B). The auto-sampler temperature was 4°C, and the injection volume was 3 μ L. The QE HFX mass spectrometer was used for its ability to acquire MS/MS spectra on information-dependent acquisition (IDA) mode in the control of the acquisition software (Xcalibur, Thermo Fisher Scientific). In this mode, the acquisition software continuously evaluates the full scan MS spectrum. The ESI source conditions were set as following: sheath gas flow rate as 30 Arb, Aux gas flow rate as 25 Arb, capillary temperature 350°C, full MS resolution as 60,000, MS/MS resolution as 7,500, collision energy as 10/30/60 in NCE mode, spray Voltage as 3.6 kV or -3.2 kV, respectively.

External metagenomic datasets of FMT

Our literature search uncovered 30 public metagenomic datasets of FMT that met the following criteria: i). public availability in September 2022; ii). sufficiently detailed description to allow unambiguous match between donors and recipients per FMT time series; iii). no restrictions on data reuse. They were included in the meta-analysis and labeled as MetS_NL_Li (n=5), MetS_NL_Kootte (n=11), UC_NL_Rossen (n=13), ABXR_NL_Singh (n=9), rCDI_AU_Schmidt (n=2), UC_AU_Schmidt (n=3), MetS_NL_Koopen (n=12), ABXR_div_Leo (n=16), ABXR_IS_BarYoseph (n=12), rCDI_US_Smillie (n=19), rCDI_US_Aggarwala (n=13), rCDI_US_Watson (n=5), rCDI_US_Podlesny (n=8), rCDI_US_Moss (n=2), UC_US_Damman (n=6), UC_US_Nusbaum (n=4), UC_US_Lee (n=2), CD_US_Vaughn (n=15), IBS_NO_Goll (n=27), MEL_US_Davar (n=15), MEL_IS_Baruch (n=10), REN_IT_Ianiro (n=7), TOU_CN_Zhao (n=5), CTR_RU_Goloshchapov (n=3), rCDI_US_Hourigan (n=9), rCDI_US_Verma (n=22), rCDI_IT_Ianiro (n=17), IBD_IT_Ianiro (n=2), ABXR_IT_Ianiro (n=5), and Obe_AU_Wilson (n=42) (Table S2).

Building an expanded SGB database

- For the in-house ASD cohort, the shotgun sequencing of total DNA from 174 fecal samples generated a total of 1,103.3 Gb quality-filtered data, which along with 1,968 public samples were included in the analyses.
- Sequencing data of the 2,142 samples were processed with the standard quality control using fastp (version 0.23.2; default parameters) and subjected to de-novo metagenomic assembly with metaSPAdes (version 3.10.1; default parameters), during which contigs shorter than 500 nt were discarded. This resulted in 1.40×10^9 different contigs with a total length of 3.00×10^{11} nt. Reads were mapped back to contigs using Bowtie2 (version 2.2.5; option '-very-sensitive-local') and the mapping output was used for contigs binning into metagenome-assembled genomes (MAGs) with MetaBAT2 (version 2.12.1; option '-m 1500'). The quality of MAGs was assessed using CheckM (version 1.0.7; default parameters), and MAGs with completeness below 50% or contamination above 5% were removed. Next, MAG redundancy was minimized by computing Mash distances on the quality-controlled assemblies, which allowed dereplication at 99.99% sequence identity and generated a total of 42,811 microbial genomes. This resource allowed us to expand the species-level genome bin (SGB) database proposed previously.³⁰ First, we used the "phylophlan_metagenomic", which is a subroutine of PhyloPhlAn 3 that applies Mash to estimate the whole-genome average nucleotide identity among genomes, to assign the 42,811 new MAGs to SGBs in the Pasolli database.³⁰ The genomes not assigned to any existing SGB (5% average genetic distance), in addition to the 64,997 reference genomes, were

organized into new SGBs spanning 5% genetic diversity using Mash (version 2.0; option “-s 1e4” for sketching) followed by hierarchical clustering with average linkage (using the fastcluster Python library). Finally, we defined 5,051 SGBs, with 1,222 of them containing at least one reference genome (kSGBs) and 3,829 containing only MAGs (uSGBs). Taxonomic assignment of SGBs profiled in this study can be found in [Table S2](#).

- We used Prokka (version 1.12, with default parameters) for functionally annotating SGBs. The annotated genomes were then processed with Roary (version 3.8, with “-e -z -g 1000000” params) for the pangenome analysis and to identify the set of core genes. The core genes (at 95% gene family clustering identity threshold) were then used as a database in PhyloPhlAn for phylogenetic analyses. Functional annotation was performed using EggNOG mapper (version 1.0.3, default parameters) based on EggNOG orthology data,¹⁰¹ and the sequence searches were performed using HMM. Functional profiles were generated with the Brite Hierarchy from KEGG, which screens metabolic-related pathways and KOs among all the KOs annotated by EggNOG. We employed the same EggNOG pipeline to functionally annotate all the 5,051 representatives of the SGBs. All the 42,811 reconstructed genomes were functionally annotated by mapping against Uniref90 and Uniref50 using Diamond (version v0.9.9.110).

QUANTIFICATION AND STATISTICAL ANALYSIS

SGB profiling of metagenomic samples

To calculate the relative abundance of SGBs, raw reads were first aligned to the representative genomes (performed using Bowtie2 as reported above). SGB relative abundance in each sample was defined as the number of reads aligning to each contig of the genome normalized by the total number of reads. Alignments were used for subsequent analyses if meeting two criteria: the alignment length was ≥ 50 nt; the edit distance between the read and the contig of genome was ≤ 2 nt.

Analysis of the association between gut microbiome features and clinical indicators or outcome

Associations of gut microbiome SGBs and KOs with clinical improvements in core ASD symptoms or GI comorbidities (negative values of ABC, CARS, and GSRS and positive value of BSFS) in the in-house ASD cohort were analyzed with Multivariate Association with Linear Model (MaAsLin) analysis, followed by Benjamini-Hochberg correction for multiple hypothesis tests. The association of clinical outcomes (responders versus non-responders) with SGB or KO transfer in 19 datasets with available outcome data was tested using LefSe analysis.

Analysis of DR intermicrobial associations

To examine the impact of donor-recipient intermicrobial interactions on engraftment, we first defined a transferred feature based on a match of SGB or KO label between a newly appeared post-FMT feature in a recipient to the same feature found in the donor (that is, present in the donor, absent in the pre-FMT recipient, and present in the post-FMT recipient). Associations between a donor SGB with pre-FMT recipient SGBs were analyzed with Spearman correlation analysis using the relative abundance data of SGBs in pre-FMT recipients and the binary presence-absence data of the donor SGB in post-FMT recipients. The effect size of major clinical and microbiome factors related to the engraftment of donor SGBs was analyzed with the adonis2 package in R software.

Analysis of mediation effects of metabolic features in-between associated SGBs and ASD indicators

To investigate the mediation effects of serum or stool metabolites in-between correlated SGBs and ASD indicators, an SGB concurrently associated with both a metabolite (MaAsLin2, FDR < 0.1) and an ASD indicator (MaAsLin2, FDR < 0.1) was identified. Next, we carried out bi-directional mediation analysis ($y = x + m + x \times m$, where y is an ASD indicator, x stands for the SGB, and m represents the mediator), in which we used the mediate function in R software (version 4.0.5) to infer the mediation effect of metabolites in-between SGBs and ASD indicators (FDR < 0.05). FDR values were calculated based on the Benjamini-Hochberg procedure using the p.adjust function in R software.

ADDITIONAL RESOURCES

The clinical trial was preregistered at Chinese Clinical Trial Registry with study ID: ChiCTR2100043906 (<https://www.chictr.org.cn/showprojEN.html?proj=122782>).